Valence One-Electron and Shake-Up Ionization Bands of Polycyclic Aromatic Hydrocarbons. III. Coronene, 1.2,6.7-Dibenzopyrene, 1.12-Benzoperylene, Anthanthrene

Michael S. Deleuze*

Departement SBG, Limburgs Universitair Centrum, Universitaire Campus, B-3590 Diepenbeek, Belgium

Received: June 25, 2004; In Final Form: August 5, 2004

A comprehensive theoretical study of the He(I) UV photoionization spectra of coronene, 1.2,6.7-dibenzopyrene, 1.12-benzoperylene, and anthanthrene up to electron binding energies of ∼18 eV is presented with the aid of one-particle Green's function calculations performed using the outer-valence Green's function (OVGF) approach and the third-order algebraic-diagrammatic construction [ADC(3)] scheme, using Dunning's correlation-consistent polarized valence basis set of double-ζ quality and the 6-31G basis set, respectively. The deviations from the one-electron OVGF/cc-pVDZ binding energies and experimental results most generally do not exceed 0.3 eV. OVGF/cc-pVDZ pole strengths smaller than 0.85 systematically corroborate a breakdown of the orbital (or one-electron) picture of ionization at the ADC(3)/6-31G level. A comparison has been made with calculations of the lowest doublet−doublet excitation energies of the related radical cations, by means of time-dependent density functional theory (TDDFT) and the Becke−Lee−Yang−Parr (BLYP) functional: Because of systematic and significant underestimations of the lowest [$\pi_0^* \leftarrow \sigma$] transition energies in the cations, this approach has led to erroneous identifications of the σ-ionization onset of the neutral molecules.

Introduction

Polycyclic aromatic hydrocarbons (PAHs) are key molecules in chemistry, physics, life, and material sciences. Over the past 15 years, evidence has been mounting to support the suggestions that PAHs account for a substantial fraction (10%) of all the interstellar carbon and are the carriers of interstellar IR absorption and emission bands in a wide variety of sources, including planetary and stellar nebula, the diffuse interstellar medium, as well as starbust galaxies.[1−3] The presence of PAHs in interstellar ices has been recently demonstrated by astronomical detection of their C−H stretching and out-of-plane bending modes in absorption in the spectra of stars embedded within dense nebular clouds.[4] High-molecular-weight PAHs have been recovered through hydropyrolysis of the carbonaceous matter contained in a giant meteorite (100 kg) that fell in Australia in 1969.[5] These compounds and their derivatives may have, therefore, been involved in the prebiotic chemical evolution that led to the emergence of life on Earth, in the form of prokaryotic cells, some 3.5×10^9 years ago.[6] Closer to our daily and terrestrial concerns, PAHs represent a major environmental issue (see refs 1, 7−10 and refs therein) because of their varied mutagenic and carcinogenic activities[11] combined with their ubiquity as combustion products of virtually all organic substances, from the burning of fuel[12] or coal to forest fires.[13] These compounds are also known as precursors of flame-produced soots[14] and fullerenes.[15,16] Last, but not least, large PAHs are very promising molecules for the manufacture of electronic devices (e.g., field effect transistors, solar cells, electroluminescent diodes) based on intrinsically well-ordered organic thin films[17] with high charge-carrier mobility.[18,19]

In many processes involving PAH compounds, radical cations play the leading role. These absorb lower-energy photons than their neutral counterparts, and a number of astrophysical observations indicate that the intense UV radiation field present in the environment ionizes a large fraction of PAHs in stellar nebula.[3] The carcinogenicity of PAHs is believed to be due to free-radical reactions and has thus been correlated with their low ionization potentials.[20] The PAH growth, as well as the formation of soot and fullerenes in hydrocarbon combustion, is known to occur by sequential additions of small acetylenic species to PAH radicals.[21] Quite naturally, therefore, the electronic excitation spectra of radical PAH cations[22] and the ionization spectra of their neutral counterparts[23−26] have received continuous attention over the last four decades. Because of the low band gap and, thus, strongly correlated character of PAHs, theoretical interpretation of these spectra represents a difficult venture, which has always lagged far behind experimentation. In particular, most of the assignments and interpretations that have been reported so far for the ultraviolet photoemission spectra (UPS) of coronene, 1.2,6.7-dibenzopyrene, 1.12-benzoperylene, and anthanthrene are very uncertain and often erroneous, because they were guided by the order of ionized states predicted by applying Koopmans' theorem upon rather modest molecular orbital (Hückel, extended Hückel, Pariser−Parr−Pople, or MNDO/2) calculations (see refs 24−26). A few years ago, K. Ohno and co-workers presented an He*(2^3S) Penning ionization study of coronene in the solid phase[27] but could not rely on better theoretical data than HF orbital energies to interpret the results of their measurements. At the level of Koopmans' theorem, misorderings of the one-electron ionization states frequently occur, caused by neglect of the electron correlation and relaxation effects. The main drawback of treatments based on the one-electron picture of ionization is that they can obviously not account for the dispersion of photoionization intensity over shake-up states corresponding to mixtures of excited configurations in the cation. For large conjugated systems in general,[28] and polycyclic aromatic hydrocarbons in particular,[29,30] there is, however, no doubt that an important part of the outer-valence ionization intensity is spread over shake-up satellites.

* Corresponding author. E-mail: deleuze@luc.ac.be.

10.1021/jp047224e CCC: $27.50
Published on Web 09/29/2004

Hirata et al. have published very recently a comprehensive study[31] of the outermost bands in the photoelectron spectra of these compounds and of many other PAHs (see also ref 22f,g), which they have assigned by comparison with calculations of the lowest excited electronic states of the related radical cations in the geometries of the neutral molecules, using time-dependent density functional theory (TDDFT)[32] in conjunction with the Becke−Lee−Yang−Parr (BLYP) functional and the 6-31G** basis set. A tacit assumption in this work is that geometrical relaxation effects are negligible, which enables a treatment of one-electron and two-electron one-hole (2h-1p) shake-up ionizations of a neutral molecule in the same fashion as one-electron transitions in the cation. This assumption is worth a check, in particular for the radical cation of coronene, which is known to be a typical Jahn−Teller species.[33] In the TDDFT study by Hirata et al.,[31] the investigated range of excitation energies did not exceed 3.0 eV. Therefore, most bands in the photoionization spectra of the title compounds have yet to be analyzed on robust-enough theoretical grounds.

An argument often invoked for not computing satellites in studies of the ionization spectra of large π-conjugated systems is that these states most generally borrow too little intensity for individually giving rise to sharp and thus easily discernible signals on the experimental side. Another argument is the assumption that only the lowest electronic configurations significantly contribute to molecular properties. Dispersion of the ionization intensity, however, over a large number of shake-up states with limited intensity may lead to considerable band broadening,[28−30,34] as well as nonnegligible contributions to the correlation background, which often complicates the interpretation of the experimental spectra. Therefore, in contrast with many semiempirical studies (e.g., see refs 35 and 36) of the ultraviolet photoemission spectra (UPS) of large π-conjugated organic molecules based on rescaled orbital energies, and in continuation of recent works on oligoacenes ranging from naphthalene to pentacene[29] and smaller angular benzologs (azulene, phenanthrene, pyrene, chrysene, triphenylene, and perylene),[30] the first purpose of the present work is to study in detail the two-hole one-particle (2h-1p) shake-up ionization bands of coronene, 1.2,6.7-dibenzopyrene, 1.12-benzoperylene (also referred to as benzo[*g*,*h*,*i*]perylene), and anthanthrene and their relationships with the one-electron ionization bands, up to electron binding energies of ∼20 eV. Also, even π-ionization bands are subject to substantial shake-up contamination,[29,30,34] an observation which motivates further assessments of the TDDFT results obtained by Hirata et al. for the lowest excited states of PAH radical cations.[31]

Methodology

To quantitatively describe such situations where the orbital (i.e., one-electron, or quasiparticle) picture of ionization breaks down, one must resort to direct theoretical methods which deal with both initial- and final-state electron correlation and, in particular, take account of configuration interactions in the cation. One of the most efficient and reliable approaches for such studies is the so-called third-order algebraic diagrammatic construction scheme [ADC(3)][37] derived within one-particle Green's function (1p-GF) theory of ionization.[38,39] At this level, the primary one-hole (1h) and two-hole one-particle (2h-1p) shake-up ionization energies are recovered through third- and first-order in electron correlation, respectively. Compared with CI treatments of ionization spectra at an equal order in electron correlation, this approach offers the key advantage of a greater compactness[40] of the matrices to be diagonalized. Moreover, unlike CI secular problems cast over a finite set of excited configurations, ADC(3) guarantees a size-consistent treatment of the ionization energies and transition moments in the limit of molecules dissociating into noninteracting fragments.[41] Size intensivity follows for large (extended) systems, provided that static self-energies are recovered from charge-consistent one-electron densities.[41] In the present work, this condition has been fulfilled by resorting to the rescaling procedure proposed in ref 42 for computing charge-consistent one-electron densities and, thus, size-intensive static self-energies through third- and fourth-order in electron correlation, respectively.

As is well-known, the major obstacles to large-scale 1p-GF/ADC(3) calculations are the exceedingly large number of ionized and excited electronic configurations spanning the secular matrices to be diagonalized and the size dependence properties of 2h-1p shake-up lines, whose number per ionized orbital scale formally like n^2 for periodic systems containing n elementary unit cells, whereas the individual intensities are proportional to n^{-2}.[41,43] All ADC(3) results presented in this work have been obtained using the original 1p-GF/ADC(3) computer package[44] interfaced to *GAMESS*,[45] which incorporates a band-Lanczos prediagonalization of the block matrices pertaining to the 2p-1h shake-on states into a pseudoelectron attachment eigenspectrum of much lower dimensions, prior to a complete block-Davidson diagonalization of the so reduced ADC(3) secular matrix.[46] All ADC(3) computations in the present study have been performed upon geometries (Figure 1) optimized at the level of density functional theory in conjunction with the Becke−three-parameters−Lee−Yang−Parr (B3LYP) functional,[47] and using Dunning's correlation-consistent polarized valence basis set of double-ζ quality (cc-pVDZ).[48] The symmetry labels presented in the sequel are consistent with the standard molecular orientations displayed in Figure 1, according to the conventions described by J. Jaffe.[49] A threshold of 0.02 on pole strengths has been retained in the final block-Davidson diagonalization step. For coronene, because of the very high symmetry of this molecule (D_{6h}), the search for eigenvalues could be extended to all shake-up lines with a pole strength larger than 0.01 in a range of binding energies extending up to 18.5 eV.

Symmetry has been exploited to the extent of the largest abelian group of the full molecular point group, and the assumption of frozen core electrons has been used throughout in order to simplify the ADC(3) calculations. Because of computational and software limitations, these calculations could not be performed with a basis set better than 6-31G. The scope of these calculations is not to calculate ionization energies within chemical accuracy (∼1 kcal mol^{-1}; that is, ∼0.04 eV) through a very accurate treatment of dynamic correlation effects, but to identify the situations where a breakdown of the orbital picture prevails and to qualitatively evaluate the extent of the shake-up contamination in both the π- and σ-ionization bands. Previous ADC(3) calculations of the ionization spectra of benzene,[29] naphthalene,[29] and azulene[30] with basis sets of improving quality (6-31G, 6-31G*, 6-31G**, cc-pVDZ, 6-311G**, ANO) have demonstrated that the ADC(3)/6-31G level is reliable enough for that purpose. More specifically, these studies have shown that the dependence of the computed ionization energies on the quality of the basis set tends to decrease rather rapidly with increasing binding energies and that successive improvements of the basis set most generally result in a redistribution of the shake-up intensity over more lines with lower intensity, but without any appreciable change in the band assignment and convoluted spectral envelopes. Even at large binding energies, the obtained sets of shake-up lines computed at the ADC(3)/

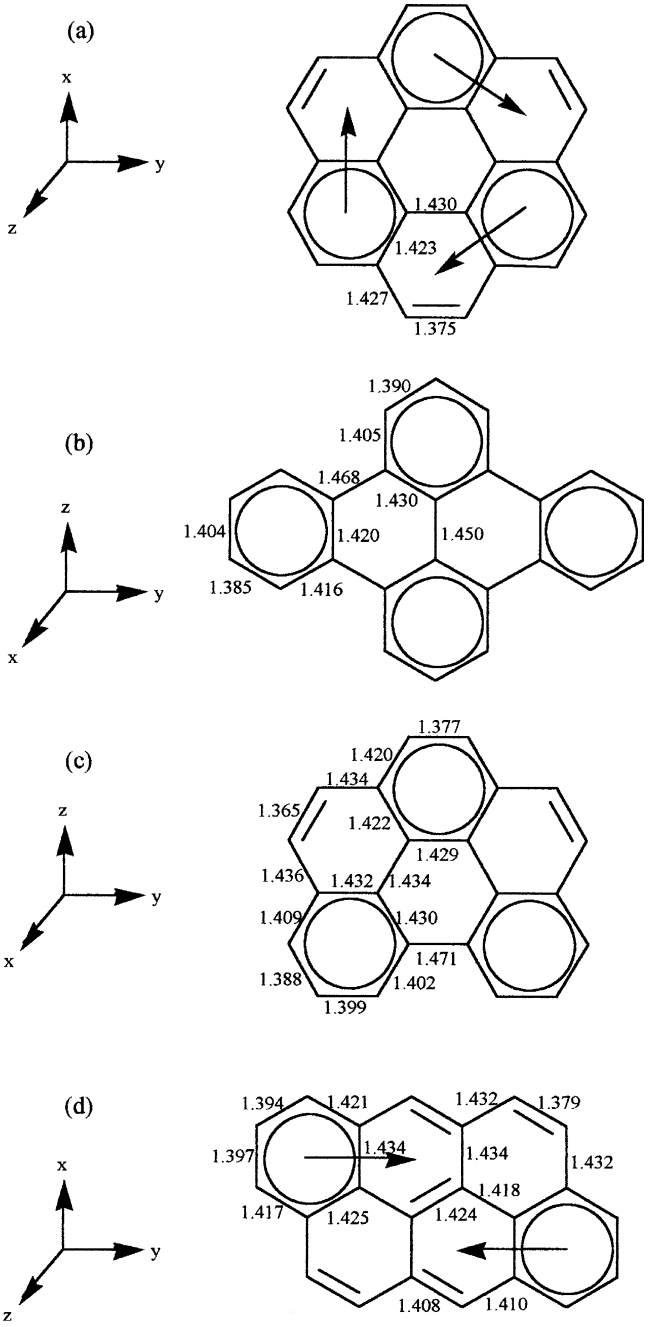

Figure 1. Clar's structure, standard molecular orientation, and details of the optimized geometry (B3LYP/cc-pVDZ bond lengths, in angstroms) of (a) coronene (D_{6h}), (b) 1.2,6.7 dibenzopyrene (D_{2h}), (c) 1.12 benzoperylene (C_{2v}), and (d) anthanthrene (C_{2h}).

6-31G level are effective densities of state which represent fair and reliable approximations of those obtained using larger basis sets. Also, the order of one-electron (Koopmans) and satellite (non-Koopmans) states lately inferred from TDDFT (BLYP)/6-31G** calculations on PAH radical cations[31] is perfectly consistent with that previously found at the ADC(3)/6-31G level for benzene, naphthalene, anthracene, tetracene, azulene, pyrene, triphenylene, chrysene, and perylene.[29,30]

In view of the limitations of the 6-31G basis set, which recovers only a small fraction of the correlation energy and poorly describes angular correlation,[50] great care is needed, however, for the ionization lines relating to the highest occupied molecular orbitals. Indeed, a benchmark focal-point analysis[51] of results obtained at theoretical levels of improving quality (HF, MP2, MP3, MP4SDQ, CCSD, CCSD(T)), along with basis

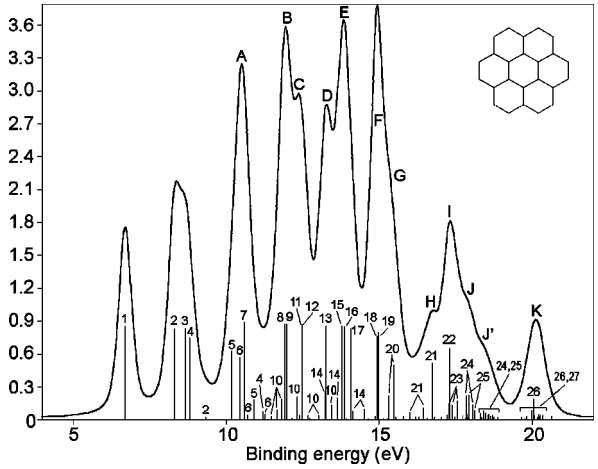

Figure 2. ADC(3)/6-31G spike and convoluted ionization spectra of coronene (fwhm = 0.5 eV).

sets of increasing size (6-31G, 6-31G*, cc-pVDZ, cc-pVTZ, cc-pVQZ), and extrapolated to the limit of an asymptotically complete (cc-pV∞Z) basis set, has shown that exceptionally large basis sets, for instance, Dunning's correlation-consistent polarized valence basis set of triple-ζ quality (cc-pVTZ),[48] are required to ensure the convergence within an accuracy of ∼0.15 eV of the vertical ionization threshold of large PAH compounds characterized by a Hartree−Fock [HF/cc-pVDZ] band gap smaller than ∼7.5 eV (such as, for instance, anthracene, naphthacene, pentacene, and hexacene). For such compounds, the stronger basis-set dependence of the outermost electron binding energies is due to the removal of dynamic correlation upon ionization, the description of which improves very slowly with the number of basis functions.[50,51] In contrast, electron binding energies obtained at the HF level upon application of Koopmans' theorem converge rapidly to their asymptotic limit.[51]

For the sake of more quantitative insights into (vertical) one-electron ionization processes, the ADC(3)/6-31G calculations have been supplemented by calculations performed using the outer-valence Green's function approach[38] and the cc-pVDZ basis set, by means of the semidirect and integral-driven algorithms incorporated into the *Gaussian98* package of programs.[52] Even with these highly efficient algorithms, OVGF calculations on the selected molecules with a larger cc-pVTZ basis set are still untractable with a powerful ES40 Compaq workstation (4 GB core memory, 100 GB disk space, dual processor 677 MHz). Like ADC(3), the OVGF approach enables the treatment of one-electron ionization energies through the third order in correlation. This approach is based on the Dyson expansion[38−42] of the one-particle Green's function in quasi-particle (i.e., diagonal) form and is thus not suited for studying shake-up processes.

Considering the intricacy of the ionization bands, which contain many and severely overlapping ionization lines, it is impossible to analyze the experimental measurements at binding energies larger than ∼10 eV without resorting to simulations drawn from the computed ADC(3) eigenspectra. As a guide to the eye, these are therefore convoluted using as a spread function a combination of a Lorentzian and Gaussian with equal weight and width (fwhm = 0.5 eV) and scaling the line intensities upon the calculated pole strengths.

Analysis of the He(I) Ionization Spectrum of Coronene. The ADC(3)/6-31G ionization energies and the related spectroscopic (pole) strengths (Γ's) obtained for coronene are displayed as spike and convoluted spectra in Figure 2 and compared with OVGF data, as well as with the experimental

TABLE 1: Results of the OVGF and ADC(3) Calculations on Coronene (D_{6h} Symmetry Point Group)[a]

level	MO	type	HF/6-31G	ADC(3)/6-31G	OVGF/6-31G	OVGF/cc-pVDZ	exptl
1	$2e_{2u}$	π	6.977	6.711 (0.854)	6.586 (0.888)	7.031 (0.879)	7.34[c]−7.36[d]
2	$2e_{1g}$	π	9.022	8.336 (0.830)	8.181 (0.880)	8.405 (0.876)	8.64[c]−8.65[d]
2	$2e_{1g}$	π [s_1][b]		9.332 (0.026)			
3	$1b_{2g}$	π	9.473	8.680 (0.836)	8.514 (0.869)	8.769 (0.862)	
3	$1b_{2g}$	π		12.147 (0.021)			
4	$1b_{1g}$	π	9.849	8.808 (0.756)[f]	8.804 (0.848)[f]	9.103 (0.838)[f]	9.15[c]−9.19[d]
4	$1b_{1g}$	π [s_3][b]		11.197 (0.083)[f]			
5	$2a_{2u}$	π	11.494	10.184 (0.636)[f]	10.182 (0.856)	10.401(0.848)[f]	10.4[c]
5	$2a_{2u}$	π [s_2][b]		10.916 (0.192)[f]			
6	$1e_{2u}$	π	12.111	10.457 (0.579)[f]	10.567 (0.829)[f]	10.803 (0.817)[f]	10.55[c]
7	$1e_{2g}$	σ	12.352	10.590 (0.894)	10.267 (0.897)	10.570 (0.888)	10.55[c]
8	$11e_{1u}$	σ	13.823	11.988 (0.879)	11.721 (0.886)	11.968 (0.876)	11.6[c]−11.8[e]
9	$5b_{2u}$	σ	13.913	11.931 (0.877)	11.592 (0.883)	11.840 (0.873)	
10	$1e_{1g}$	π	14.170	12.330 (0.216)[f]	12.185 (0.806)[f]	12.366 (0.793)[f]	
11	$3a_{2g}$	σ	14.344	12.491 (0.867)	12.284 (0.879)	12.467 (0.870)	∼12.4[e]
12	$6b_{1u}$	σ	14.349	12.468 (0.871)	12.240 (0.882)	12.548 (0.868)	
13	$10e_{2g}$	σ	15.367	13.263 (0.858)	12.998 (0.874)	13.198 (0.864)	∼13.3[e]
14	$1a_{2u}$	π	15.734	13.242 (0.278)[f]	13.421 (0.776)[f]	13.548 (0.758)[f]	
15	$4b_{2u}$	σ	15.891	13.773 (0.863)	13.507 (0.879)	13.644 (0.870)	∼13.6[e]
16	$10e_{1u}$	σ	15.971	13.873 (0.856)	13.631 (0.873)	13.773 (0.863)	∼13.6[e]
17	$8a_{1g}$	σ	16.118	14.064 (0.839)	13.871 (0.870)	14.036 (0.860)	
18	$9e_{1u}$	σ	17.272	14.943 (0.772)	14.745 (0.861)	14.909 (0.850)	∼14.9[e]
19	$9e_{2g}$	σ	17.197	14.967 (0.802)	14.824 (0.863)	14.993 (0.852)	∼14.9[e]
20	$8e_{2g}$	σ	17.752	15.465 (0.505)[f]	15.252 (0.845)[f]	15.311 (0.832)[f]	
21	$7a_{1g}$	σ	19.170	16.727 (0.525)[f]	16.335 (0.831)[f]	16.375 (0.817)[f]	∼16.8[e]
22	$3b_{2u}$	σ	19.739	17.283 (0.661)[f]	16.978 (0.817)[f]	16.997 (0.802)[f]	
23	$8e_{1u}$	σ	20.102	17.274 (0.150)[f]	17.303 (0.820)[f]	17.340 (0.806)[f]	
24	$5b_{1u}$	σ	20.748	17.833 (0.230)[f]	17.838 (0.815)[f]	*f*	
25	$2a_{2g}$	σ	21.085	17.926 (0.234)[f]	18.124 (0.813)[f]	*f*	
26	$6a_{1g}$	σ	23.102	20.040 (0.198)[f]	*f*	*f*	
27	$7e_{2g}$	σ	23.482	19.979 (0.060)[f]	*f*	*f*	

[a] Binding energies are given in eV, along with the associated pole strengths (Γ's) in brackets. [b] [s_x] dominant shake-up configuration: $s_1 = 2e_{2u}^{-2}\ 3e_{1g}^{+1}$ (doubly degenerate HOMO^{-2} LUMO^{+1} state, correlating with the $2a_{1u}^{-2}\ 4b_{2g}^{+1}$ and $4b_{1u}^{-2}\ 4b_{3g}^{+1}$ electronic configuration upon a D_{2h} point group); $s_2 = 2e_{2u}^{-2}\ 3e_{2u}^{+1}$ (non degenerate HOMO^{-2} (LUMO + 1)$^{+1}$ state, correlating with the $2a_{1u}^{-1}\ 4b_{1u}^{-1}\ 4b_{3g}^{+1}$ electronic configuration within a D_{2h} point group); $s_3 = 2e_{2u}^{-2}\ 3e_{1g}^{+1}$ (nondegenerate HOMO^{-2} LUMO^{+1} state, correlating with the $2a_{1u}^{-1}\ 4b_{1u}^{-1}\ 3a_{1u}^{+1}$ electronic configuration within a D_{2h} point group). [c] Value reported by Boschi, R.; Murell, J. N.; Schmidt, W. *Discuss. Faraday Soc.* **1972**, *54*, 116. [d] Value reported by Boschi, R.; Schmidt, W. *Tetrahedron Lett.* **1972**, 2577 or by Boschi, R.; Clar, E.; Schmidt, W. *J. Chem. Phys.* **1974**, *60*, 4406. [e] Value obtained from the rescaled He(I) and PIE spectra provided by Yanakado, H.; Sawada, Y.; Shonohara, H.; Ohno, K. *J. Electron Spectrosc. Relat. Phenom.* **1998**, *88*, 927. [f] Breakdown of the molecular orbital picture of ionization. At binding energies larger than 12.5 eV, only the most intense ADC(3)/6-31G ionization lines are given here; see Table 2 for further data.

He(I) results by Boshi and Smith[25] in Table 1. These calculations place the vertical ionization threshold at 6.7 eV, in very reasonable agreement, considering the limited size of the employed basis set, with the experimental value (7.34 eV). Clearly, the orbital picture of ionization prevails for the highest ocupied molecular orbital (HOMO, in this case, $2e_{2u}$), and the vertical ionization threshold can thus be evaluated more quantitatively by means of the OVGF/cc-pVDZ approach. At this level, the first ionization potential does not deviate from the experimental value by more than 0.31 eV. This was not entirely unexpected, considering the HF/cc-pVDZ band gap (8.58 eV) of coronene, which is comparable with that of azulene (8.39 eV), anthracene (8.48 eV), and pyrene (8.65 eV). For these three molecules, the agreement between the vertical OVGF/cc-pVDZ value and the experimental ionization thresholds was within ∼0.24 to ∼0.37 eV (see Table 1 in ref 51). Some care is needed, however, because coronene$^+$ is known to be a typical Jahn−Teller species.[33] An adiabatic ionization threshold of 6.91 eV is obtained upon adding to the OVGF/cc-pVDZ value (7.03 eV) the B3LYP/cc-pVDZ corrections for geometrical relaxation effects (−0.064 eV) and changes in (harmonic) zero-point vibrational energies (−0.054 eV). In the He(I) spectrum of Boschi and Schmidt [25] (Figure 3), the $2e_{2u}$ ionization band (**1**) of coronene takes the form of a very asymmetric vibrational progression, characterized by a sharp onset at 7.34 eV.

As was already noted in ref 30, the agreement between OVGF and experimental values improves with increasing binding energies. The peak (**2**) at a binding energy of 8.64 eV in the He(I) spectrum (Figure 3a) very clearly relates to the ionization of an electron from the $2e_{1g}$ (**2**) orbital. Taking into account a theoretical energy interval of ∼0.35 eV between the $2e_{1g}^{-1}$ (**2**) and $1b_{2g}^{-1}$ (**3**) ionization lines, it can reasonably be expected that the onset of the $1b_{2g}^{-1}$ (**3**) ionization band lies at ∼9.00 eV. Thus, clearly, the peak at ∼8.8 eV in Figure 3a relates to a vibronic transition induced by the ionization of orbital $2e_{1g}$ (**2**). In the π-band system of coronene, the lowest identified shake-up transition (s_1) lies at a relatively low binding energy (9.3 eV), comparable with that found for PAH compounds with a similar band gap (azulene, $s_1 = 9.6$ eV; anthracene, $s_1 = 10.4$ eV; pyrene, $s_1 = 9.5$ eV). The ADC(3) results indicate a slight breakdown of the orbital picture for the ionization of an electron in orbital $1b_{1g}$ (**4**), in the form of a shake-up line at 11.2 eV with a nonnegligible pole strength (0.08). The extent of the shake-up fragmentation intensifies with the ionization of orbitals $2a_{2u}$ (**5**) and $1e_{2u}$ (**6**). In all cases, this breakdown can be foretold by a drop of the OVGF/cc-pVDZ pole strength below 0.85, an observation which also prevails for the remaining π-orbitals and throughout the σ-band system of coronene (Tables 1 and 2). Ionization of the (nondegenerate) π-orbital $2a_{2u}$ (**5**) yields a shake-up line at 10.9 eV ($\Gamma = 0.19$), which falls within the vibrational tail of the (doubly degenerate) $1e_{2u}^{-1}$ and $1e_{2g}^{-1}$ ionization lines (**6** and **7**, respectively).

The one-electron picture of ionization is fully recovered with the $1e_{2g}$ orbital (**7** in Figure 3), which defines the σ-ionization

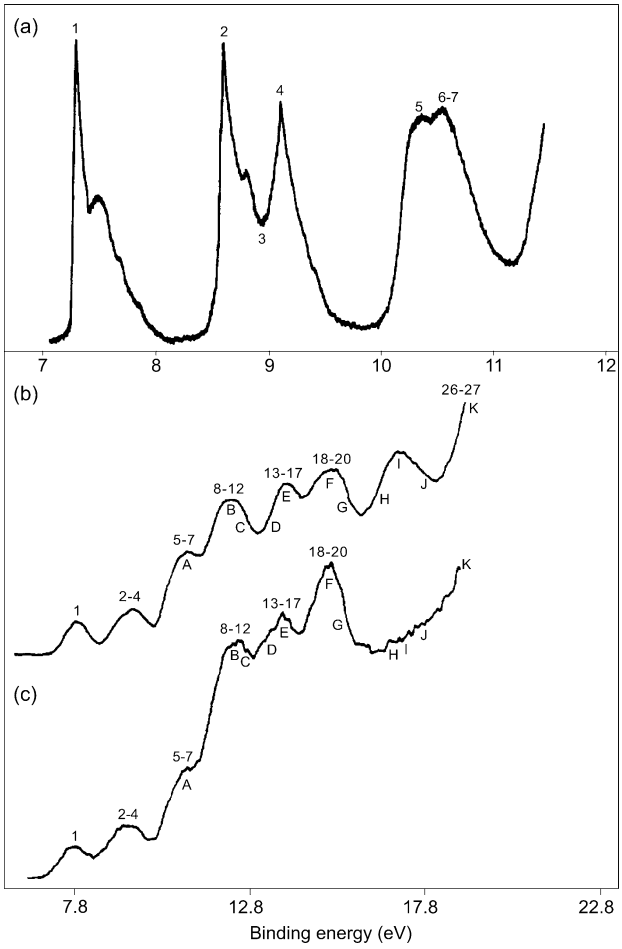

Figure 3. Experimental ionization spectra of coronene. (a) Gas-phase He(I) measurements (adapted from ref 25). (b) PIE and (c) He(I) measurements in the solid phase (adapted from ref 27).

onset. In contrast to the π-ionization threshold, and despite (or possibly because of) the neglect of vibronic coupling effects, the fit between theory (OVGF/cc-pVDZ) and experiment [He(I)] is almost perfect for that orbital. The comparison is, at first glance, less satisfactory for the $11e_{1u}$ (**8**) and $5b_{2u}$ (**9**) σ-orbitals. For these orbitals, the OVGF/cc-pVDZ results (12.0, 11.8 eV) rather significantly overestimate the ultimate value (11.6 eV) reported in ref 25. It is worth noting that the origin of this experimental value is very uncertain, because in their original study,[25] Boschi and Schmidt apparently did not investigate electron binding energies larger than 11.5 eV (see Figure 3a). It must also be noted that the $11e_{1u}^{-1}$ and $5b_{2u}^{-1}$ ionization lines (**8**, **9**) overlap with shake-up lines originating from the π-orbital $1e_{1g}$ (**10**). The ADC(3) results indicate that, for this orbital, the breakdown of the one-electron picture of ionization is complete (Table 1). The recovered $1e_{1g}$ (**10**) shake-up ionization intensity is found in a binding energy range of 11.7−15.1 eV (Table 2) and thus is far beyond the next two σ one-electron ionization lines ascribed to orbitals $3a_{2g}$ (**11**) and $6b_{1u}$ (**12**). Similarly, ionization of the lowest-lying π-orbital ($1a_{2u}$, **14**) yields a number of shake-up lines at binding energies ranging from 12.4 to 18.4 eV (Table 2).

In the σ-band system of coronene, the one-electron picture of ionization remains valid up to electron binding energies of ∼15 eV (Table 1). Therefore, six intense and rather sharp peaks (**A**-**F**) should be seen (Figure 2) in gas-phase He(I) measurements on this molecule, at binding energies of ∼10.58 (**7**), ∼11.9 (**8**, **9**), ∼12.5 (**11**, **12**), ∼13.2 (**13**), ∼13.8 (**15**−**17**), and ∼15.0 eV (**18**, **19**); see Table 1 for a detailed orbital assignment.

TABLE 2: Further Ionization Lines Identified at the ADC(3)/6-31G Level for Coronene (D_{6h} Symmetry Point Group)[a]

level	MO	type	ADC(3)/6-31G
4	$1b_{1g}$	π	11.905 (0.008), 13.919 (0.015), 14.037 (0.011), 14.799 (0.005)
5	$2a_{2u}$	π	11.987 (0.023), 16.233 (0.010), 16.913 (0.007)
6	$1e_{2u}$	π	10. 718 (0.049), 11.284 (0.061), 11.818 (0.196), 11.485 (0.033), 11.871 (0.007), 12.384 (0.045), 12.672 (0.043), 12.721 (0.019), 13.666 (0.008), 14.058 (0.012), 14.648 (0.012), 14.739 (0.009)
10	$1e_{1g}$	π	10.523 (0.006), 11.670 (0.095), 12.663 (0.042), 13.020 (0.046), 13.426 (0.140), 13.792 (0.012), 13.921 (0.007), 14.528 (0.017), 14.875 (0.042), 15.130 (0.020), 15.463 (0.007)
14	$1a_{2u}$	π	12.350 (0.010), 12.993 (0.006), 13.625 (0.205), 14.137 (0.084), 14.516 (0.102), 14.863 (0.029), 15.268 (0.017), 15.533 (0.031), 15.565 (0.012), 16.160 (0.012), 16.451 (0.011), 16.569 (0.020), 17.119 (0.009), 17.222 (0.010), 18.210 (0.006), 18.360 (0.011), 18.546 (0.007)
19	$9e_{2g}$	σ	16.790 (0.025)
20	$8e_{2g}$	σ	15.312 (0.227), 15.791 (0.038), 16.203 (0.034)
21	$7a_{1g}$	σ	16.008 (0.071), 16.297 (0.036), 16.436 (0.121), 19.752 (0.025)
22	$3b_{2u}$	σ	16.441 (0.046), 16.807 (0.032)
23	$8e_{1u}$	σ	17.029 (0.031), 17.212 (0.052), 17.374 (0.144), 17.470 (0.037), 17.553 (0.177), 17.818 (0.021), 17.901 (0.025), 18.330 (0.021), 18.367 (0.022)
24	$5b_{1u}$	σ	17.724 (0.038), 18.060 (0.146), 18.111 (0.095), 18.345 (0.033), 18.413 (0.088)
25	$2a_{2g}$	σ	17.869 (0.060), 18.311 (0.068), 18.477 (0.072), 18.555 (0.051), 18.586 (0.055), 18.652 (0.037), 18.691 (0.049), 18.755 (0.028), 18.885 (0.030)
26	$6a_{1g}$	σ	19.644 (0.029), 19.814 (0.037), 19.975 (0.096), 20.209 (0.060), 20.243 (0.043), 20.631 (0.041)
27	$7e_{2g}$	σ	20.073 (0.046), 20.168 (0.032), 20.168 (0.033), 20.253 (0.050), 20.317 (0.036), 20.333 (0.034), 20.340 (0.050)

[a] Binding energies are given in eV, along with the associated pole strengths (Γ's) in brackets.

A significant band broadening is expected for orbitals $8e_{2g}$ (**20**) and $7a_{1g}$ (**21**), with regard to the rather limited spectroscopic strengths (0.51, 0.53) of the most intense lines identified for these orbitals in the theoretical ADC(3) spike spectrum (Table 1) and a dispersion of the remaining ionization intensity over several shake-up lines (Table 2). In the convoluted spectrum (Figure 2), orbital $8e_{2g}$ (**20**) appears as a shoulder (**G**) on peak **F**, at a binding energy around 15.5 eV, whereas the most intense line due to ionization of orbital $7a_{1g}$ (**21**) is partially resolved (peak **H**) at ∼16.5 eV.

The PIE (Penning ionization electron) and He(I) spectra recorded by K. Ohno and co-workers on coronene in the solid phase[27] are reproduced and assigned in Figure 3b and c, respectively. These spectra are fully consistent with the theoretical simulation of Figure 2, taking into account the fact that further band broadening is expected on the experimental side because of intermolecular interactions. In these figures, the PIE and UPS measurements by K. Ohno[27] have been shifted down by 2.8 eV, to align the position of the most intense peak (**F**) in He(I) on the OVGF results for the $9e_{1u}$ (**18**) and $9e_{2g}$ (**19**) orbitals, and thereby implicitly account for the work function of solid coronene, as well as solid-state polarization effects, which are assumed to have a constant influence on all ionized states. The binding energies obtained for all other bands through this rescaling are in excellent agreement with the 1p-GF theoretical data (Table 1). In particular, the σ-ionization onset is located at ∼11.8 eV (maximum of band **A**) and thus is 0.2 eV above the value reported by Boschi and Smith.[25] This

assignment is consistent with the reduced collision-energy dependence of the partial ionization cross section ($m = -0.01$ au meV^{-1}) of this band with mixed σ- and π-character in the PIE spectrum of coronene,[27] compared with that of the two bands relating to the π-levels ($m = -0.08$ au meV^{-1} and $m = -0.13$ au meV^{-1}). In the rescaled solid-state spectra (Figure 3b, c), these lines are found at binding energies around ~9.1 and ~7.6 eV, respectively. We note also that, in these PIE and He(I) spectra (Figure 3b,c), and in line with the simulation of Figure 2, the band **B** has a shoulder **C** on its high binding energy side, whereas a shoulder **D** precedes peak **E**.

The innermost line which still partially exhibits some one-hole character ($\Gamma = 0.66$) in the ADC(3)/6-31G ionization spectrum of coronene (Table 1) is a line that originates from orbital $3b_{2u}$ (**22**), at 17.3 eV. The related peak (**I**) in the convolution of Figure 2 is followed by two shoulders (**J**, **J′**) at binding energies of ~18.0 and ~18.5 eV, which are due to shake-up lines relating to orbitals $8e_{1u}$ (**23**), $5b_{1u}$ (**24**), and $2a_{2g}$ (**25**). Another shoulder (**H**) marks the presence of the most important line associated to orbital $7a_{1g}$ (**21**) at ~16.4 eV. Despite the extent of the shake-up contamination in this energy region (Table 2), the ADC(3)/6-31G results (Figure 3a) are fully consistent with the rescaled PIES measurements by K. Ohno and co-workers[27] in the solid phase (Figure 3b), which exhibit an intense and asymmetric signal (**H**, **I**, **J**) around ~16.8 eV. In view of the LCAO composition of the $5b_{1u}$ (**24**) and $2a_{2g}$ (**25**) orbitals, the (**J**, **J′**) shoulders define the top of the inner-valence (C_{2s}) region. The composition of these shoulders explains the enhanced and positive collision energy dependence of the partial ionization cross section ($m = 0.11$ au meV^{-1})[27] pertaining to the band around ~16.8 eV in the shifted PIE spectrum, which reflects the more localized and thus less accessible nature of orbitals $5b_{1u}$ (**24**) and $2a_{2g}$ (**25**) in chemi-ionization processes under collision with an He*(2^3S) atomic probe.

The ultimate peak (**K**) displayed in the simulation of Figure 2, at ~20.0 eV, is due to a number of shake-up lines (Table 2) with extremely limited intensities and relating to the inner-valence orbitals $6a_{1g}$ (**26**) and $7e_{2g}$ (**27**). It is worth recalling that, for coronene, because of the very slow convergence of the block-Davidson iterations for shake-up states at binding energies larger than 18.5 eV, only the lines with a pole strength larger than 0.03 could be recovered in this energy region. It is, therefore, quite certain that the peak that should be seen at ~20 eV in a gas-phase He(II) spectrum of coronene also encompasses shake-up lines derived from the ionization of one further C_{2s} orbital $7e_{1u}$ (**28**). Indeed, this orbital has an HF/6-31G energy of 23.52 eV, very close to that of orbital $7e_{2g}$ (**27**), and many satellites should have presumably been found for that orbital around ~20.0 eV in the ADC(3)/6-31G spectrum, if the search could have been extended to lines with pole strengths smaller than 0.03.

It is worth mentioning that the ADC(3)/6-31G calculations locate the (doubly degenerate) $2e_{1g}^{-1}$ (**2**), $1b_{2g}^{-1}$ (**3**), and $1b_{1g}^{-1}$ (**4**) ionization lines of coronene in its $^1A_{1g}$ ground state (D_{6h} symmetry) at 1.63, 1.97, and 2.10 eV above the ionization threshold, $2e_{2u}^{-1}$ (**1**), respectively. In view of the stronger dependence of the ionization threshold on the size of the basis set, these results are qualitatively in line with the first excitation energies calculated by Hirata et al. [31] by means of TDDFT (BLYP)/6-31G** calculations on coronene$^+$ in its neutral geometry, and the ^2A_u ground state under the constraint of a D_{2h} point group (despite the fact that, as with any monodeterminantal treatment of intrinsically multideterminantal wave functions, the latter calculations are subject to a (nonphysical) symmetry breaking (SB) of the Kohn−Sham electron density and, thus, releases of orbital degeneracies).[31] With this approach, the obtained doublet−doublet excitation energies amount to 1.14 and 1.21 eV for the SB split $^2B_{3g}$ [$\pi_0^* \leftarrow \pi_{-2}$] and $^2B_{2g}$ [$\pi_0^* \leftarrow \pi_{-3}$] states, 1.65 eV for the $^2B_{3g}$ [$\pi_0^* \leftarrow \pi_{-4}$] state, and 1.69 eV for the $^2B_{2g}$ [$\pi_0^* \leftarrow \pi_{-5}$] state of coronene$^+$,[53] to compare with experimental excitation energies of 1.31 and 1.47, 1.62, and 1.77 eV, respectively.[54] The most quantitative insights into the lowest excitation energies of coronene$^+$ are obtained at the OVGF/cc-pVDZ level, which places the $2e_{1g}^{-1}$ (**2**) and $1b_{2g}^{-1}$ (**3**) ionization lines of coronene at 1.37 and 1.74 eV above the first $2e_{2u}^{-1}$ ionization line. Taking into account the fact that the ionization of a spin-down electron in orbital $2e_{2u}$ and the subsequent Jahn−Teller distortion of the molecular geometry of coronene into a structure of D_{2h} symmetry induces a B3LYP/cc-pVDZ splitting by ~0.12 eV of the spin-down components of the $2e_{1g}$ pair, one obtains ultimately the values of 1.31 and 1.43 eV (1.37 ± 0.06 eV) for the $^2B_{3g}$ [$\pi_0^* \leftarrow \pi_{-2}$] and $^2B_{2g}$ [$\pi_0^* \leftarrow \pi_{-3}$] excitation energies of coronene$^+$,[53] in almost perfect agreement with the above listed experimental values. The comparison between the OVGF and TDDFT results would be irrelevant for the $1b_{1g}$ (**4**), $2a_{2u}$ (**5**), and $1e_{2u}$ (**6**) orbitals, because for these orbitals, both the OVGF/cc-pVDZ and ADC(3)/6-31G results consistently prove that the one-electron picture of ionization breaks down (Table 1). The ADC(3)/6-31G energy separations between the $2e_{2u}^{-1}$ (**1**) line and the most intense lines derived from the ionization of orbitals $1b_{1g}$ (**4**), $2a_{2u}$ (**5**), and $1e_{2u}$ (**6**) are 2.10, 3.47, and 3.75 eV, to compare with experimental He(I) values of 1.81, 3.06, and 3.21 eV, respectively. There are no TDDFT (BLYP)/6-31G** results reported in the work by Hirata et al.[31] for the corresponding [$\pi_0^* \leftarrow \pi$] doublet excited states of coronene$^+$, namely $^2B_{2g}$, $^2B_{1u}$, and {^2A_u + $^2B_{1u}$}.[53] The OVGF/cc-pVDZ (ADC(3)/6-31G) calculations locate the outermost one-electron σ-ionization line [$1e_{2g}^{-1}$ (**7**)] at 3.77 (3.88) eV above the ionization threshold, to compare with an experimental He(I) energy interval of 3.21 and a TDDFT (BLYP)/6-31G** value of 2.90 eV for the $^2B_{1g}$ [$\pi_0^* \leftarrow \sigma_{-1}$] excitation energy in coronene$^+$.[53] Passing by, in view of the obtained ADC(3)/6-31G and OVGF/cc-pVDZ results, two slight errors in the work on coronene$^+$ by Hirata et al.[31] can be corrected. In their assignment, the $^2B_{3g}$ [$\pi_0^* \leftarrow \pi_{-4}$] and $^2B_{1g}$ [$\pi_0^* \leftarrow \sigma_{-1}$] states of coronene$^+$ (under a D_{2h} point group[53]) have been incorrectly associated with experimental electron binding energies at 1.83 and 3.0 eV above the $2e_{2u}^{-1}$ (**1**) ionization energy. According to Table 1, these values define the positions of the $1b_{1g}$ (**4**) and $2a_{2u}$ (**5**) ionization bands relative to the ionization threshold of coronene and, with regard to the MO correlations between the respective point groups, should have been compared with the $^2B_{2g}$ [$\pi_0^* \leftarrow \pi_{-5}$] (1.69 eV) and $^2B_{1u}$ [$\pi_0^* \leftarrow \pi_{-6}$] (unreported) excitation energies of coronene$^+$ (D_{2h}),[53] respectively.

Analysis of the He(I) Ionization Spectrum of 1.2,6.7-Dibenzopyrene. By virtue of its large (D_{2h}) symmetry point group, the convoluted ADC(3) spectrum of 1.2,6.7-dibenzopyrene (Figure 4) exhibits a number of well-resolved peaks and bands, overall in irrefutably excellent agreement with experimental values (Figure 5, Table 3). This molecule has a HF/cc-pVDZ band gap of 9.01 eV, significantly larger than that of coronene (8.58 eV), pyrene (8.65 eV), or naphthacene (7.28 eV), which can be related to the lower chemical reactivity of this molecule[55] and its more strongly benzenoid and thus aromatic nature (see, in particular, Table 15 and the analysis thereby on p 3496 in ref 55; see also the B3LYP/cc-pVDZ bond

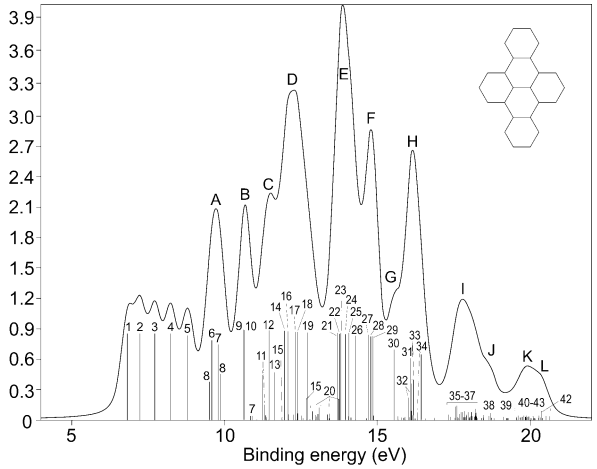

Figure 4. ADC(3)/6-31G spike and convoluted ionization spectra of 1.2,6.7-dibenzopyrene (fwhm = 0.5 eV).

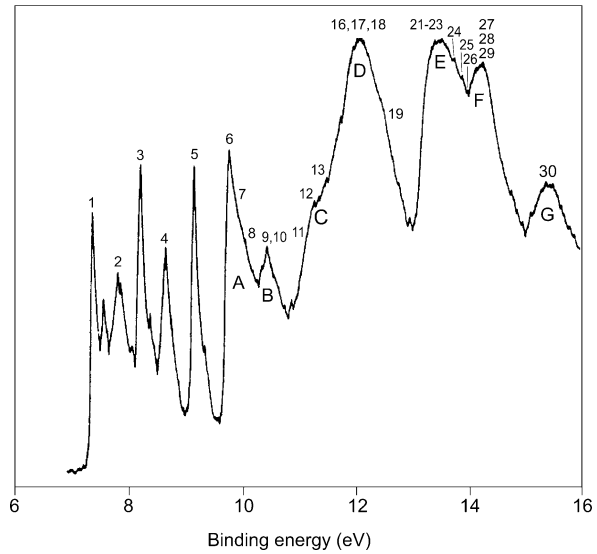

Figure 5. Gas-phase He(I) photoemission spectrum of 1.2,6.7-dibenzopyrene (adapted from ref 26).

lengths displayed in Figure 1, which verify the bond equalization expected for the π-sextet rings[55−58] of polycyclic aromatic hydrocarbons). Quite naturally, therefore, the first ionization energy of 1.2,6.7-dibenzopyrene is very accurately calculated at the OVGF/cc-pVDZ level. An adiabatic ionization threshold of 7.06 eV, 0.34 eV below the experimental value, is obtained upon adding to the OVGF/cc-pVDZ value (7.13 eV) the B3LYP/cc-pVDZ corrections for geometrical relaxation effects (−0.060 eV) and changes in (harmonic) zero-point vibrational energies (−0.011 eV). One peak is seen at ∼7.6 eV in the He(I) spectrum by Boschi et al.,[26] which belongs to the vibrational tail of the $3b_{1g}^{-1}$ (**1**) ionization line. The next four peaks (**2**−**5**) in the He(I) spectrum undoubtedly relate to one-electron ionization processes (see Table 3 for details). Their energy locations can thus also be accurately calculated at the OVGF/cc-pVDZ level, within an accuracy range of 0.3−0.4 eV. The ionization lines found for the $3b_{3u}$ (**6**) and $2b_{1g}$ (**7**) π-orbitals represent borderline cases, with regard to the calculated OVGF/cc-pVDZ pole strengths (0.850 and 0.856). A slight dispersion of the $3b_{3u}$ (**6**) and $2b_{1g}$ (**7**) ionization intensities into secondary processes is correspondingly observed at the ADC(3)/6-31G level. The OVGF/cc-pVDZ results seem to contradict the breakdown of the orbital picture of ionization which the ADC(3)/6-31G level predicts for the $1a_u$ orbital (**8**). An OVGF/cc-pVDZ pole strength significantly larger than 0.85 is obtained for that orbital, whereas two lines with comparable intensities (Γ = 0.38 and 0.46) are found at binding energies of ∼9.5 and ∼9.9 eV in the ADC(3)/6-31G spectrum. The former ionization energy defines the shake-up onset (s_1) in the π-band system of dibenzopyrene. It is worth noting that the relative intensities ascribed to the outermost shake-up lines of PAHs can also be rather sensitive to the basis set (see, in particular, the results displayed for the $1b_{1g}$ (**4**) orbital of naphthalene in Figure 4 and Table 3 of ref 29, or for the $1a_2$ (**3**) orbital of azulene in Figure 1 and Table 1 of ref 30; in view of these results,[29,30] on the other hand, it is worth noting that the energy location of the shake-up onset (s_1) appears to be relatively insensitive to the basis set). Therefore, a reasonable explanation to this contradiction between ADC and OVGF is that the 6-31G basis set might lead to an overestimation of the fraction of intensity which is ascribed to the s_1 satellite. Beyond this point, drops of OVGF/cc-pVDZ pole strengths below the empirical threshold of ∼0.85 always foretell a significant dispersion of the ionization intensity over shake-up lines at the ADC(3) level, or a complete breakdown of the orbital picture of ionization (see Tables 3 and 4).

The outermost σ-levels are reached with peak **B** at 10.47 eV. This band relates to the one-electron ionization lines that originate from two nearly degenerate levels, $20a_g$ (**9**) and $14b_{3g}$ (**10**), which explains the unusually sharp appearance of that peak in the σ-region. A shoulder (**C**) is seen at ∼11.3 eV in the He(I) spectrum, which, according to the ADC(3)/6-31G and OVGF/cc-pVDZ results, can be ascribed to a few lines originating from ionization of the $2b_{3u}$ and $1b_{2g}$ π-orbitals (**11**, **13**), as well as to a one-electron ionization line ascribed to the $16b_{2u}$ σ-orbital (**12**). Convolution of the next four σ one-electron ionization lines relating to orbitals $17b_{1u}$ (**14**), $15b_{2u}$ (**16**), $19a_g$ (**17**), and $13b_{3g}$ (**18**) corroborates the broad and intense band (**D**) culminating at ∼12.2 eV in the He(I) spectrum. This band also encompasses a series of shake-up lines (Table 4) related to the $1b_{1g}$ (**15**) π-level, at binding energies ranging from 12.0 to 14.1 eV. In line with the OVGF/cc-pVDZ result for the σ-orbital $16b_{1u}$ (**19**), a slight shoulder can be discerned experimentally on the right-hand side of band **D**, at a binding energy of ∼12.7 eV.

As orbital $1b_{1g}$ (**15**), the innermost π-level of dibenzopyrene, namely, $1b_{3u}$ (**20**), is also subject to a complete breakdown of the orbital picture of ionization, in the form of many shake-up lines at binding energies ranging from ∼12.5 to ∼16.9 eV (Table 4), and most certainly beyond. In excellent agreement with experimental results, the convoluted ADC(3)/6-31G spectrum exhibits two rather sharp peaks (**E** and **F**) at binding energies of ∼13.5 and ∼14.3 eV relating to the **21**−**26** and **27**−**29** subsets of one-electron ionization lines (see Table 3 for a detailed orbital assignment). A peak of lower intensity (**G**) is ultimately seen at a binding energy of ∼15.4 eV in the He(I) spectrum (Figure 5), which can also be assigned to an ionization line with a rather large pole strength (Γ = 0.70), and relating to the $14b_{1u}$ orbital (**30**). This line possesses a few satellites with rather significant intensities (Table 4). Beyond this point, the shake-up fragmentation intensifies in the σ-band system, and the OVGF approach can no longer be reliably applied.

The one-electron picture of ionization is still partly preserved for orbitals $12b_{2u}$ (**31**) and $11b_{2u}$ (**34**), in the forms of two lines at binding energies of ∼16.1 and ∼16.4 eV and pole strengths larger than 0.60 in the ADC(3)/6-31G spectrum (Table 3), which together with a number of shake-up lines derived from orbitals $15a_g$ (**32**) and $13b_{1u}$ (**33**) yield a sharp peak at ∼16.3 eV in the convoluted spectrum displayed in Figure 4. Two broader bands (**I** and **K**) are also seen in this simulation at ∼17.7 and ∼19.8

TABLE 3: Results of the OVGF and ADC(3) Calculations on Dibenzopyrene (D_{2h} Symmetry Point Group)[a]

level	MO	type	HF/6-31G	ADC(3)/6-31G	OVGF/6-31G	OVGF/cc-pVDZ	exptl[b]
1	$3b_{1g}$	π	7.189	6.835 (0.857)	6.707 (0.888)	7.130 (0.879)	7.40
2	$3b_{2g}$	π	7.646	7.251 (0.859)	7.116 (0.889)	7.379 (0.884)	7.83
3	$2a_u$	π	8.296	7.732 (0.848)	7.608 (0.882)	7.876 (0.875)	8.24
3	$2a_u$	π [s_4][e]		11.083 (0.011)			
4	$4b_{3u}$	π	8.857	8.246 (0.857)	8.102 (0.886)	8.328 (0.880)	8.67
5	$2b_{2g}$	π	9.565	8.803 (0.839)	8.693 (0.878)	8.952 (0.871)	9.19
6	$3b_{3u}$	π	10.707	9.607 (0.792)	9.546 (0.860)	9.797 (0.850)	9.84
6	$3b_{3u}$	π [s_5][e]		11.897 (0.032)			
7	$2b_{1g}$	π [s_2][e]	10.919	9.808 (0.749)	9.779 (0.864)	10.024 (0.851)	10.0[c]
7	$2b_{1g}$	π [s_3][e]		10.875 (0.043)			
7	$2b_{1g}$	π		10.922 (0.041)			
8	$1a_u$	π [s_1][e]		9.522 (0.383)[d]			
8	$1a_u$	π	10.663	9.895 (0.457)[d]	9.585 (0.871)	9.804 (0.864)	
9	$20a_g$	σ	12.375	10.635 (0.893)	10.364 (0.898)	10.645 (0.888)	10.47[c]
10	$14b_{3g}$	σ	12.467	10.677 (0.894)	10.372 (0.898)	10.660(0.888)	10.47[c]
11	$2b_{3u}$	π	13.143	11.271 (0.448)[d]	11.380 (0.820)[d]	11.598 (0.808)[d]	11.3[c]
12	$16b_{2u}$	σ	13.217	11.471 (0.886)	11.261 (0.894)	11.531 (0.883)	11.3[c]
13	$1b_{2g}$	π	13.582	11.644 (0.473)[d]	11.687 (0.809)[d]	11.872 (0.796)[d]	11.3[c]
14	$17b_{1u}$	π	13.804	11.971 (0.880)	11.736 (0.889)	11.976 (0.878)	
15	$1b_{1g}$	π	14.232	11.972 (0.267)[d]	12.302 (0.814)[d]	12.467 (0.802)[d]	
16	$15b_{2u}$	σ	13.998	12.082 (0.877)	11.812 (0.885)	12.044 (0.874)	12.2[c]
17	$19a_g$	σ	14.165	12.337 (0.876)	12.129 (0.888)	12.358 (0.877)	12.2[c]
18	$13b_{3g}$	σ	14.265	12.384 (0.870)	12.203 (0.884)	12.440 (0.872)	12.2[c]
19	$16b_{1u}$	σ	14.594	12.711 (0.865)	12.545 (0.881)	12.778 (0.869)	12.7[c]
20	$1b_{3u}$	π	15.453	13.738 (0.214)[d]	*d*	13.344 (0.770)[d]	
21	$14b_{2u}$	σ	15.858	13.698 (0.864)	13.447 (0.877)	13.589 (0.866)	13.5[c]
22	$15b_{1u}$	σ	15.755	13.765 (0.857)	13.610 (0.879)	13.782 (0.868)	13.5[c]
23	$18a_g$	σ	15.874	13.801 (0.862)	13.558 (0.878)	13.666 (0.868)	13.5[c]
24	$13b_{2u}$	σ	16.049	13.960 (0.848)	13.685 (0.874)	13.818 (0.863)	
25	$12b_{3g}$	σ	16.250	14.077 (0.861)	13.849 (0.877)	13.967 (0.867)	
26	$11b_{3g}$	σ	16.404	14.289 (0.835)	14.095 (0.872)	14.230 (0.860)	
27	$17a_g$	σ	16.940	14.710 (0.842)	14.494 (0.869)	14.569 (0.858)	14.3[c]
28	$10b_{3g}$	σ	16.954	14.792 (0.827)	14.617 (0.866)	14.804 (0.855)	14.3[c]
29	$16a_g$	σ	17.011	14.854 (0.830)	14.678 (0.869)	14.877 (0.858)	14.3[c]
30	$14b_{1u}$	σ	17.802	15.530 (0.699)[d]	15.462 (0.855)	15.549 (0.843)[d]	15.4[c]
31	$12b_{2u}$	σ	18.506	16.077 (0.613)[d]	*d*	15.902 (0.832)[d]	
32	$15a_g$	σ	18.508	16.112 (0.365)[d]	16.016 (0.844)[d]	*d*	
33	$13b_{1u}$	σ	18.516	16.172 (0.403)[d]	*d*	*d*	
34	$11b_{2u}$	σ	18.785	16.423 (0.656)[d]	*d*	*d*	
35	$14a_g$	σ	20.151	17.596 (0.146)[d]	*d*	*d*	
36	$12b_{1u}$	σ	20.723	17.836 (0.095)[d]	*d*	*d*	
37	$9b_{3g}$	σ	20.932	18.194 (0.114)[d]	*d*	*d*	
38	$10b_{2u}$	σ	21.371	18.688 (0.079)[d]	*d*	*d*	
39	$13a_g$	σ	22.580	19.591 (0.046)[d]	*d*	*d*	
40	$11b_{1u}$	σ	23.180	19.781 (0.047)[d]	*d*	*d*	
41	$8b_{3g}$	σ	23.387	20.083 (0.043)[d]	*d*	*d*	
42	$12a_g$	σ	23.414	20.359 (0.095)[d]	*d*	*d*	
43	$9b_{2u}$	σ	23.912	20.270 (0.045)[d]	*d*	*d*	

[a] Binding energies are given in eV, along with the associated pole strengths (Γ's) in brackets. [b] Boschi, R.; Clar, E.; Schmidt, W. *J. Chem. Phys.* **1974**, *60*, 4406. [c] My assignment. [d] Breakdown of the molecular orbital picture of ionization. At binding energies larger than 12.5 eV, only the most intense ADC(3)/6-31G ionization lines are given here; see Table 4 for further data. [e] [s_x] dominant shake-up configuration: $s_1 = 3b_{1g}^{-2}\,3a_u^{+1}$; $s_2 = 3b_{1g}^{-2}\,4b_{1g}^{+1}$; $s_3 = 3b_{1g}^{-1}\,2a_u^{-1}\,3a_u^{+1}$; $s_4 = 2a_u^{-2}\,a_u^{+1} + 3b_{1g}^{-1}\,2a_u^{-1}\,4b_{1g}^{+1}$; $s_5 = 3b_{2g}^{-2}\,5b_{3u}^{+1}$.

eV. These bands can be ascribed to dense sets of shake-up lines with average pole strengths smaller than 0.05 and which borrow their intensities from the **35**−**37** and **40**−**43** orbital subsets (see Tables 3 and 4 for details). Most of these orbitals belong to the inner-valence band system (the top of the C_{2s} region coincides with orbital $12b_{1u}$ (**36**)). At last, two shoulders (**J** and **L**) are predicted, at ∼18.7 and ∼20.4 eV, and mark the presence in this energy region of slightly more intense shake-up lines ($\Gamma >$ 0.08) derived from ionization of the $10b_{2u}$ (**38**) and $12a_g$ (**42**) orbitals (Table 4).

The OVGF/cc-pVDZ (ADC(3)/6-31G) calculations place the $3b_{2g}^{-1}$ (**2**), $2a_u^{-1}$ (**3**), $4b_{3u}^{-1}$ (**4**), $2b_{2g}^{-1}$ (**5**), $3b_{3u}^{-1}$ (**6**), $2b_{1g}^{-1}$ (**7**), and $20a_g^{-1}$ (**9**) ionization lines at 0.25 (0.42), 0.75 (0.90), 1.20 (1.41), 1.82 (1.97), 2.67 (2.77), 2.89 (2.97), and 3.52 (3.80) eV above the ionization threshold [$3b_{1g}^{-1}$ (**1**)] of 1.2,6.7-dibenzopyrene, to compare with experimental He(I) energy intervals of 0.43, 0.84, 1.27, 1.79, 2.44, 2.60, and 3.07 eV, respectively. These results are in line with the TDDFT (BLYP)/6-31G** calculations by Hirata et al. [31]on the related radical cation, which locate the $^2B_{2g}$, ^2A_u, $^2B_{3u}$, $^2B_{2g}$, $^2B_{3u}$, $^2B_{1g}$, and ^2A_g doublet excited states of 1.2,6.7-dibenzopyrene$^+$ at 0.30, 0.57, 1.24, 1.32, 2.17, 2.28, and 2.52 eV above the electronic ground state ($^2B_{1g}$).[53] Again, however, the present analysis for the σ-ionization onset [$20a_g^{-1}$ (**9**)] of 1.2,6.7-dibenzopyrene differs from that reported in ref 31. In their work, Hirata et al. have assigned this onset to a peak at ∼2.5 eV above the $3b_{1g}^{-1}$ (**1**) line. Very clearly (Table 3, Figure 4), this peak (**A**) exclusively relates to the ionization of π-orbitals (vide supra), and the TDDFT (BLYP)/6-31G** value of 2.52 eV reported by Hirata et al. for the ^2A_g [$\pi_0^* \leftarrow \sigma_{-8}$] excitation energy should have been compared with an experimental value of 3.07 eV, which correctly defines the position of the σ-ionization onset (peak **B**, MOs **9** and **10** in Table 3) relative to the π-ionization threshold. At the TDDFT (BLYP)/6-31G** level, only one

TABLE 4: Further Ionization Lines Identified at the ADC(3)/6-31G Level for Dibenzopyrene (D_{2h} Symmetry Point Group)[a]

level	MO	type	ADC(3)/6-31G
3	$2a_u$	π	11.982 (0.008), 12.311 (0.008)
8	$1a_u$	π	12.569 (0.010), 12.800 (0.010)
11	$2b_{3u}$	π	11.314 (0.155), 11.381 (0.033), 12.393 (0.076)
13	$1b_{2g}$	π	11.314 (0.072), 11.363 (0.052), 13.067 (0.068), 13.424 (0.024)
15	$1b_{1g}$	π	12.101 (0.060), 12.255 (0.059), 12.572 (0.025), 12.692 (0.218), 13.029 (0.041), 14.132 (0.031)
20	$1b_{3u}$	π	13.099 (0.130), 12.526 (0.047), 12.886 (0.094), 12.979 (0.058), 13.373 (0.063), 13.441 (0.066), 14.060 (0.045), 14.636 (0.023), 14.870 (0.045), 16.864 (0.026)
30	$14b_{1u}$	σ	15.676 (0.043), 15.865 (0.028), 15.896 (0.037)
31	$12b_{2u}$	σ	15.798 (0.025), 16.175 (0.050), 16.427 (0.031)
32	$15a_g$	σ	16.010 (0.224), 16.163 (0.052), 16.222 (0.022), 16.314 (0.082)
33	$13b_{1u}$	σ	16.120 (0.329)
34	$11b_{2u}$	σ	16.039 (0.031), 16.093 (0.097)
35	$14a_g$	σ	17.320 (0.057), 17.540 (0.137), 17.549 (0.039), 17.586 (0.050), 17.620 (0.030), 17.666 (0.025), 17.686 (0.066), 17.731 (0.086), 17.845 (0.030), 17.916 (0.055)
36	$12b_{1u}$	σ	17.376 (0.034), 17.523 (0.025), 17.635 (0.032), 17.735 (0.078), 17.814 (0.037), 17.893 (0.048), 17.955 (0.084), 17.994 (0.022), 18.066 (0.028), 18.451 (0.022)
37	$9b_{3g}$	σ	17.785 (0.084), 18.016 (0.034), 18.069 (0.083), 18.107 (0.044), 18.177 (0.035), 18.219 (0.074), 18.272 (0.024)
38	$10b_{2u}$	σ	18.049 (0.049), 18.167 (0.021), 18.228 (0.036), 18.401 (0.021), 18.446 (0.029), 18.473 (0.056), 18.637 (0.046), 18.647 (0.045), 18.696 (0.077), 18.723 (0.028), 18.811 (0.023)
39	$13a_g$	σ	19.123 (0.034), 19.206 (0.021), 19.252 (0.024), 19.267 (0.022), 19.539 (0.035), 19.548 (0.025), 19.656 (0.033), 19.726 (0.036), 19.854 (0.046), 19.883 (0.031), 19.906 (0.035), 19.995 (0.023), 20.257 (0.025)
40	$11b_{1u}$	σ	19.825 (0.034), 19.832 (0.034)
41	$8b_{3g}$	σ	19.942 (0.039), 20.015 (0.022), 20.105 (0.022), 20.312 (0.028)
42	$12a_g$	σ	20.116 (0.023), 20.157 (0.023), 20.356 (0.025), 20.385 (0.025)
43	$9b_{2u}$	σ	20.497 (0.044), 20.634 (0.037)

[a] Binding energies are given in eV, along with the associated pole strengths (Γ's) in brackets.

^2A_u state has been found,[31] at 2.28 eV above the $^2B_{1g}$ ground state of 1.2,6.7-dibenzopyrene$^+$. This corroborates the OVGF/cc-pVDZ results for orbital $1a_u$ (**8**), described at the latter level as a one-electron ionization line ($\Gamma = 0.864$) at 2.67 eV, but contradicts the ADC(3)/6-31G calculations (Table 3) which predict two lines with comparable intensities ($\Gamma = 0.38$ and 0.46) at 2.69 and 3.05 eV above the ionization threshold. Clearly, ADC(3) calculations with larger basis sets will be necessary to clarify this issue.

Analysis of the He(I) Ionization Spectrum of 1.12-Benzoperylene. The ADC(3)/6-31G ionization spectrum of 1.12-benzoperylene displayed in Figure 6 exhibits many similarities to that of coronene (Figure 2). 1.12-Benzoperylene has a HF/cc-pVDZ band gap of 8.11 eV, intermediate to that of perylene (7.59 eV) and coronene (8.58 eV). This band gap is thus large enough to ensure a calculation of its vertical ionization threshold within an accuracy of ~0.4 eV at the OVGF/cc-pVDZ level (Table 5). The experimental He(I) value of 7.19 eV must be more correctly compared with an adiabatic ionization threshold of 6.76 eV, obtained by taking into account the B3LYP/cc-pVDZ corrections of −0.067 and +0.007 eV for the geometrical relaxation effects and changes in zero-point harmonic vibrational energies, respectively. Only three of the six one-electron ionization lines relating to the π-levels of 1.12-benzoperylene, namely, $5a_2$ (**1**), $6b_1$ (**2**), and $4b_1$ (**6**), are individually resolved experimentally, along with the associated vibrational progressions. On the other hand, three partly resolved structures at 8.70, 8.85, and 9.05 in the He(I) spectrum (Figure 7) have been assigned by Boschi et al.[24] to the $4a_2$ (**3**), $5b_1$ (**4**), and $3a_2$ (**5**) orbitals, respectively, on the basis of very elementary molecular orbital calculations. For all of these lines, the agreement between the OVGF/cc-pVDZ values and the measured binding energies is excellent, around 0.3 eV, with the exception of orbital $3a_2$ (**5**), for which an unusually large discrepancy of 0.44 eV is noticed if we assume that the original assignment by Boschi et al.[24] is correct. It can also be noticed that, at both the ADC(3)/6-31G and OVGF/cc-pVDZ levels, the energy spacing between the $5b_1^{-1}$ (**4**) and $3a_2^{-1}$ (**5**) ionization lines does not exceed 0.08 eV (at the HF level, the corresponding orbitals are quasidegenerate). It is thus much more reasonable to ascribe the peak at 8.85 eV in the He(I) spectrum (Figure 7) to both the $5b_1$ (**4**) and $3a_2$ (**5**) orbitals and invoke vibronic coupling interactions to explain the origin of the peak at 9.05 eV. This suggestion is further supported by the larger width of the peak at 8.85 eV in the He(I) spectrum, in comparison with the very sharp vibrational onsets which characterize the $5a_2^{-1}$ (**1**), $6b_1^{-1}$ (**2**), $4a_2^{-1}$ (**3**), and $4b_1^{-1}$ (**6**) ionization bands.

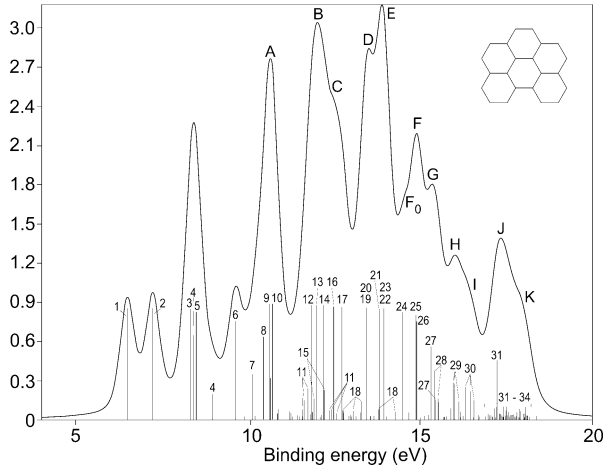

Figure 6. ADC(3)/6-31G spike and convoluted ionization spectra of 1.12-benzoperylene (fwhm = 0.5 eV).

The ADC(3)/6-31G results (Table 5) indicate a significant dispersion of the $5b_1$ (**4**) photoionization intensity into a rather strong satellite at 9.0 eV ($\Gamma = 0.20$), which represents the shake-up onset (s_1) of 1.12-benzoperylene. However, a pole strength of 0.865 is found at the OVGF/cc-pVDZ level for the $5b_1$ (**4**) level, which seems to indicate that the orbital picture of ionization could be (at least partly) recovered for that level if ADC(3) calculations with larger basis sets could be performed. For all other orbitals, OVGF/cc-pVDZ pole strengths smaller than 0.85 consistently foretell a breakdown of the orbital picture of ionization at the ADC(3)/6-31G level (Tables 5 and 6). Ionization of the $3b_1$ (**7**) π-level yields an intense shake-up line [$\Gamma = 0.35$] at 10.1 eV in the ADC(3)/6-31G spectrum. A partial breakdown of the orbital picture of ionization is noticed for the next π-level, $2a_2$ (**8**). At binding energies beyond 10.5 eV, the orbital picture of ionization fully breaks down in the π-band system.

Both the OVGF/cc-pVDZ and ADC(3)/6-31G calculations place the σ-ionization threshold at 10.63−10.70 eV (**9**, **10**),

TABLE 5: Results of the OVGF and ADC(3) Calculations on Benzo[*g,h,i*]perylene (C_{2v} Symmetry Point Group)[a]

level	MO	type	HF/6-31G	ADC(3)/6-31G	OVGF/6-31G	OVGF/cc-pVDZ	exptl
1	$5a_2$	π	6.733	6.500 (0.854)	6.381 (0.888)	6.824 (0.880)	7.19
2	$6b_1$	π	7.617	7.237 (0.852)	7.115 (0.887)	7.532 (0.879)	7.86
3	$4a_2$	π	8.971	8.328 (0.853)	8.174 (0.882)	8.407 (0.877)	8.70
4	$5b_1$	π	9.258	8.428 (0.652)[d]	8.416 (0.871)	8.675 (0.865)	8.85
4	$5b_1$	π [s_1][e]		8.982 (0.196)[d]			9.2[b]
5	$3a_2$	π	9.256	8.502 (0.829)	8.364 (0.874)	8.608 (0.867)	8.85[b,c]
5	$3a_2$	π [s_2][e]		9.902 (0.026)			
6	$4b_1$	π	10.771	9.630 (0.758)	9.582 (0.855)	9.834 (0.844)[d]	9.88
7	$3b_1$	π [s_4][e]	11.700	10.134 (0.351)[d]	10.363 (0.848)[d]	10.582 (0.839)[d]	10.3[b]
7	$3b_1$	π [s_5][e]		10.651 (0.322)[d]			
8	$2a_2$	π [s_3][e]		10.213 (0.033)[d]			
8	$2a_2$	π	11.985	10.455 (0.643)[d]	10.498 (0.832)[d]	10.742 (0.821)[d]	10.3[b]
9	$32a_1$	π	12.386	10.641 (0.894)	10.329 (0.898)	10.625 (0.888)	10.58
10	$29b_2$	π	12.455	10.712 (0.894)	10.413 (0.897)	10.701 (0.888)	10.58
11	$2b_1$	π	13.666	11.755 (0.239)[d]	*d*	11.978 (0.796)[d]	11.2[b]
12	$31a_1$	π	13.725	11.856 (0.878)	11.592 (0.887)	11.841 (0.876)	11.9[b]
13	$28b_2$	π	13.825	12.004 (0.876)	11.764 (0.886)	12.007 (0.875)	12.0[b]
14	$30a_1$	π	14.091	12.198 (0.875)	11.917 (0.884)	12.157 (0.873)	12.2[b]
15	$1a_2$	π	14.140	12.220(0.195)[d]	12.189 (0.807)[d]	12.367 (0.794)[d]	
16	$27b_2$	π	14.381	12.499 (0.866)	12.299 (0.881)	12.536 (0.869)	12.5[b]
17	$26b_2$	π	14.611	12.731 (0.864)	12.555 (0.879)	12.799 (0.868)	12.7[b]
18	$1b_1$	π	15.549	13.443(0.150)[d]	13.303 (0.768)[d]	13.433 (0.736)[d]	13.1[b]
19	$25b_2$	σ	15.520	13.445 (0.862)	13.178 (0.878)	13.360 (0.867)	13.4[b]
20	$29a_1$	σ	15.474	13.446 (0.855)	13.252 (0.877)	13.444 (0.866)	13.4[b]
21	$28a_1$	σ	15.903	13.826 (0.848)	13.595 (0.876)	13.743 (0.866)	
22	$27a_1$	σ	16.026	13.950 (0.827)	13.736 (0.874)	13.866 (0.864)	13.7[b]
23	$24b_2$	σ	16.078	13.951 (0.856)	13.692 (0.873)	13.822 (0.863)	13.7[b]
24	$26a_1$	σ	16.734	14.504 (0.828)	14.230 (0.866)	14.375 (0.856)	14.4[b]
25	$23b_2$	σ	17.104	14.884 (0.803)	14.707 (0.865)	14.876 (0.853)	15.0[b]
26	$25a_1$	σ	17.140	14.908 (0.757)	14.796 (0.863)	14.967 (0.853)	15.0[b]
27	$24a_1$	σ	17.629	15.320 (0.561)[d]	15.225 (0.851)[d]	15.299 (0.838)[d]	15.5[b]
28	$22b_2$	σ	17.777	15.421 (0.379)[d]	15.320 (0.847)[d]	15.381 (0.835)[d]	15.5[b]
29	$21b_2$	σ	18.390	15.965 (0.287)[d]	15.896 (0.844)	15.972 (0.831)[d]	
30	$23a_1$	σ	18.932	16.322 (0.253)[d]	*d*	*d*	
31	$22a_1$	σ	19.753	17.249 (0.457)[d]	*d*	*d*	
32	$21a_1$	σ	20.040	17.522 (0.105)[d]	*d*	*d*	
33	$20b_2$	σ	20.355	17.893 (0.086)[d]	*d*	*d*	
34	$19b_2$	σ	20.813	18.074 (0.100)[d]	*d*	*d*	

[a] Binding energies are given in eV, along with the associated pole strengths (Γ's) in brackets. [b] My assignment. [c] Originally assigned to a peak at 9.05 eV by Boschi et al. [d] Breakdown of the molecular orbital picture of ionization. At binding energies larger than 10.0 eV, only the most intense ADC(3)/6-31G ionization lines are given here; see Table 6 for further data. [e] [s_x] dominant shake-up configuration: $s_1 = 5a_2^{-2}\ 7b_1^{+1}$; $s_2 = 6b_1^{-2}\ 6a_2^{+1}$; $s_3 = 5a_2^{-2}\ 7a_2^{+1}$; $s_4 = 5a_2^{-2}\ 9b_1^{+1}$; $s_5 = 5a_2^{-2}\ 9b_1^{+1}$.

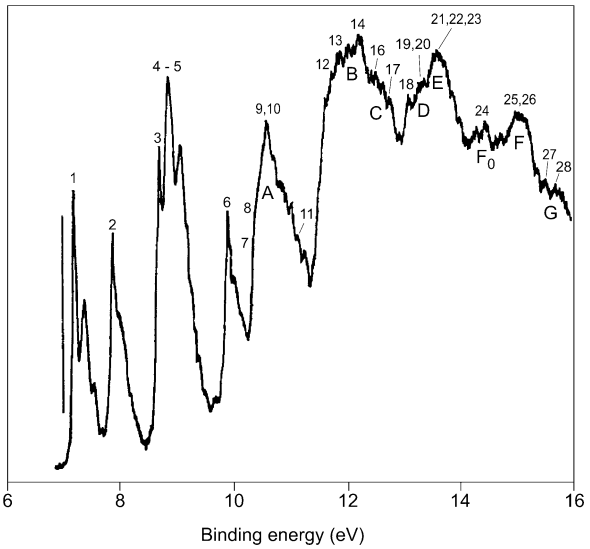

Figure 7. Gas-phase He(I) photoemission spectrum of 1.12-benzoperylene (adapted from ref 24).

again in almost perfect agreement with experimental results (10.58 eV). In the He(I) spectrum (Figure 7), an unusually broad shoulder is clearly discerned at ~10.3 eV, thus at 0.3 eV below the σ-onset which coincides with the extremum of band **A**. The next spectral feature seen experimentally (Figure 7) is a band (**B**) around 12 eV. This band exhibits three substructures at 11.9, 12.0, and 12.2 eV, which, in view of the ADC(3)/6-31G and OVGF/cc-pVDZ results (Figure 6, Table 5), can be confidently ascribed to the one-electron ionization lines derived from the $31a_1$ (**12**), $28b_2$ (**13**), and $30a_1$ (**14**) σ-orbitals. In agreement with the convoluted ADC(3)/6-31G spectrum (Figure 6), band **B** in the He(I) spectrum (Figure 7) is followed by one shoulder (**C**) at 12.5−12.7 eV, which relates (Table 5) to one-electron ionization lines derived from the $27b_2$ (**16**) and $26b_2$ (**17**) σ-orbitals. A number of shake-up lines belonging to the π-band system also appear in this binding energy range (Figure 6, Table 6), which borrow their intensities from orbitals $2b_1$ (**11**), $1a_2$ (**15**), and $1b_1$ (**18**).

In an analogy with the ADC(3)/6-31G spectrum of coronene (see Figure 2), and in excellent agreement with experimental results (Figure 7), the **B**−**C** band complex of 1.12-dibenzopyrene (Figure 6) is mirrored by another pair of bands (**D**−**E**) extending over a binding energy range between 13 and 14 eV. Here, the shoulder (**D**, at 13.4 eV) lies at a lower binding energy than the band extremum (**E**, at 13.7 eV). These spectral features can be ascribed to one-electron ionization lines relating to the {$25b_2$ (**19**), $29a_1$ (**20**)} and {$28a_1$ (**21**), $27a_1$ (**22**), $24b_2$ (**23**)} orbital subsets, respectively. The only σ-ionization line that can be resolved experimentally (band $\mathbf{F_0}$ at 14.4 eV) derives from

TABLE 6: Further Ionization Lines Identified at the ADC(3)/6-31G Level for Benzo[*g,h,i*]perylene (C_{2v} Symmetry Point Group)[a]

level	MO	type	ADC(3)/6-31G
7	$3b_1$	π	10.879 (0.081), 11.213 (0.069), 11.263 (0.054)
8	$2a_2$	π	10.213 (0.033), 11.451 (0.034), 11.597 (0.026)
11	$2b_1$	π	11.651 (0.148), 10.854 (0.050), 11.584 (0.080), 11.880 (0.059), 12.582 (0.050), 12.793 (0.055), 13.069 (0.068), 13.144 (0.028), 14.504 (0.027)
15	$1a_2$	π	11.924 (0.161), 11.300 (0.023), 11.517 (0.024), 11.827 (0.044), 12.108 (0.025), 12.386 (0.074), 12.428 (0.083), 12.984 (0.039), 13.021 (0.025), 13.288 (0.058)
18	$1b_1$	π	12.149 (0.035), 12.770 (0.073), 12.941 (0.032), 13.316 (0.142), 13.561 (0.031), 13.669 (0.030), 13.805 (0.084), 13.961 (0.045), 14.281 (0.063)
22	$27a_1$	σ	14.030 (0.029)
25	$23b_2$	σ	15.018 (0.021)
26	$25a_1$	σ	15.135 (0.034)
27	$24a_1$	σ	15.453 (0.157), 15.695 (0.026), 15.779 (0.030)
28	$22b_2$	σ	15.265 (0.039), 15.530 (0.163), 15.542 (0.138), 15.713 (0.023), 16.016 (0.025)
29	$21b_2$	σ	15.895 (0.093), 16.004 (0.240), 16.126 (0.132)
30	$23a_1$	σ	16.172 (0.063), 16.192 (0.022), 16.247 (0.034), 16.466 (0.221), 16.547 (0.023), 16.566 (0.140), 16.686 (0.039), 16.906 (0.024)
31	$22a_1$	σ	16.716 (0.026), 17.036 (0.037), 17.177 (0.087), 17.326 (0.052)
32	$21a_1$	σ	17.424 (0.103), 16.976 (0.047), 17.222 (0.099), 17.337 (0.049), 17.487 (0.034), 17.498 (0.075), 17.584 (0.061), 17.616 (0.026)
33	$20b_2$	σ	17.115 (0.027), 17.202 (0.022), 17.337 (0.031), 17.386 (0.037), 17.404 (0.027), 17.436 (0.023), 17.516 (0.026), 17.535 (0.035), 17.550 (0.039), 17.647 (0.039), 17.684 (0.039), 17.747 (0.026), 17.823 (0.062), 17.879 (0.021), 18.027 (0.021), 18.095 (0.034), 18.098 (0.032), 18.193 (0.024)
34	$19b_2$	σ	17.717 (0.045), 17.734 (0.045), 17.779 (0.023), 17.801 (0.034), 17.927 (0.069), 17.932 (0.040), 18.010 (0.048), 18.047 (0.054), 18.116 (0.036), 18.130 (0.032), 18.398 (0.032)

[a] Binding energies are given in eV, along with the associated pole strengths (Γ's) in brackets.

orbital $26a_1$ (**24**). A broader and more intense band (**F**) is seen experimentally at 15.0 eV; this band is due to the $23b_2^{-1}$ and $25a_1^{-1}$ σ-ionization lines (**25**, **26**). Beyond this point, the orbital picture of ionization starts to break down in the σ-band system (Tables 5 and 6). Thus, the shoulder (**G**) that is ultimately seen at 15.5 eV in the He(I) spectrum of 1.12-benzoperylene (Figure 7) most certainly relates to shake-up lines (Tables 5 and 6) which find their origin in the ionization of orbitals $24a_1$ (**27**) and $22b_2$ (**28**).

In the theoretical convolution of Figure 6, the shake-up contributions from the next two orbitals (**29**, **30**), namely, $21b_2$ and $23a_1$, fall in a clearly distinct band (**H**) culminating at 16.0 eV and which is followed by a shoulder (**I**) at 16.4 eV that more specifically relates to orbital $23a_1$ (**30**). Proceeding further, the breakdown of the one-electron picture of ionization intensifies for orbitals $22a_1$ (**31**), $21a_1$ (**32**), $20b_2$ (**33**), and $19b_2$ (**34**), which fully belong to the C_{2s} band system. Ionization of these orbitals results in many shake-up lines with, overall, extremely limited intensities ($\Gamma < 0.10$), at binding energies ranging from 16.7 up to (at least) 18.4 eV (Tables 5 and 6). In this energy region, a very noteworthy feature (Table 5) is a rather intense line at 17.2 eV in the ADC(3)/6-31G spectrum ($\Gamma = 0.46$), which borrows its ionization intensity from orbital $22a_1$ (**31**).

The OVGF/cc-pVDZ (ADC(3)/6-31G) calculations locate the $6b_1^{-1}$ (**2**), $4a_2^{-1}$ (**3**), $5b_1^{-1}$ (**4**), $3a_2^{-1}$ (**5**), and $4b_1^{-1}$ (**6**) ionization lines at 0.71 (0.74), 1.58 (1.83), 1.85 (1.93), 1.78 (2.00), and 3.00 (3.13) eV above the ionization threshold [$5a_2^{-1}$ (**1**)] of 1.12-benzoperylene, to compare with the TDDFT (BLYP)/6-31G** estimates[31] of 0.60, 1.39, 1.71, 1.73, and 2.38 eV for the $^2B_1$ [$\pi_0^* \leftarrow \pi_{-1}$], $^2A_2$ [$\pi_0^* \leftarrow \pi_{-2}$], $^2B_1$ [$\pi_0^* \leftarrow \pi_{-3}$], $^2A_2$ [$\pi_0^* \leftarrow \pi_{-4}$], and $^2B_1$ [$\pi_0^* \leftarrow \pi_{-5}$] doublet−doublet excitation energies of 1.12-benzoperylene$^+$ in its $^2A_2$ ground state, respectively. Electronic absorption measurements correspondingly place the $^2A_2$ [$\pi_0^* \leftarrow \pi_{-2}$], $^2B_1$ [$\pi_0^* \leftarrow \pi_{-3}$], and $^2A_2$ [$\pi_0^* \leftarrow \pi_{-4}$] states of this radical cation at excitation energies of 1.51, 1.62, and 1.84 eV.[54] It thus appears that the OVGF/cc-pVDZ method provides the most accurate insights into the $^2A_2$ [$\pi_0^* \leftarrow \pi_{-2}$] and $^2A_2$ [$\pi_0^* \leftarrow \pi_{-4}$] excitation energies of 1.12-benzoperylene$^+$ but rather strongly overestimates the $^2B_1$ [$\pi_0^* \leftarrow \pi_{-3}$] excitation energy. This failure of the OVGF approach stems from the partial breakdown of the one-electron picture of ionization which the ADC(3)/6-31G level predicts for the $5b_1$ orbital (**4**) and, thus, the presence at nearby energies of shake-up states that can mix with the $5b_1^{-1}$ one-hole configuration. It is worth noting that the energy order inferred from the ADC(3)/6-31G one-electron ionization energies of 1.12-benzoperylene for the six lowest doublet excited states of 1.12-benzoperylene$^+$ is, this time, entirely consistent with that obtained by Hirata et al.[31] In particular, the shake-up onset (s_1), relating to the $5a_2^{-2}$ $7b_1^{+1}$ (HOMO^{-2} LUMO^{+1}) satellite (s_1) of the $5b_1^{-1}$ (**4**) ionization line, is found at 2.48 eV above the ionization threshold in the ADC(3)/6-31G spectrum of 1.12-benzoperylene, in line with the TDDFT (BLYP)/6-31G** calculations by Hirata et al. which assign a band at 2.40−2.47 eV in the electronic absorption spectrum of 1.12-benzoperylene$^+$ to a $^2B_1$ [$\pi_1^* \leftarrow \pi_0$] state at an excitation energy of 2.67 eV. A value of 2.84 eV has been reported by Hirata et al. for the $^2A_1$ [$\pi_0^* \leftarrow \sigma_{-1}$] excitation energy of 1.12-benzoperylene$^+$, to compare with energy separations of 4.14, 3.80, and 3.45 eV between the π- and σ-ionization onsets in the ADC(3)/6-31G, OVGF/cc-pVDZ, and He(I) ionization spectra of 1.12-dibenzopyrene, respectively.

Analysis of the He(I) Ionization Spectrum of Anthanthrene. In comparison with 1.12-benzoperylene, enhanced shake-up fragmentation is noticed in the ionization spectrum of anthanthrene (Table 7, Figure 8), an observation which corroborates the reduced band gap ($E_g = 6.81$ eV, at the HF/cc-pVDZ level), lesser aromatic (Figure 1d, see also refs 55 and 58) and, thus, more reactive nature of this compound. In line with this reduced band gap, the OVGF/cc-pVDZ calculation underestimates the ionization threshold of anthanthrene (**1**) by as much as 0.61 eV. For the sake of comparison, discrepancies of 0.44, 0.48, and 0.54 eV have been previously reported between the OVGF/cc-pVDZ and He(I) ionization thresholds of naphthacene ($E_g = 7.28$ eV), pentacene ($E_g = 6.40$ eV), and hexacene ($E_g = 5.74$ eV), respectively.[29,51] Including B3LYP/cc-pVDZ corrections for geometrical relaxation effects (−0.061 eV) and changes in harmonic zero-point vibrational energies (+0.016 eV) leads to an adiabatic ionization potential of 6.27 eV, which is still 0.65 eV below the experimental ionization threshold. In view of our recent benchmark focal-point study on large oligoacenes,[51] the only way at present to significantly improve the theoretical determination of this threshold would be to use much larger basis sets, such as cc-pVTZ (828 MOs) or even cc-pVQZ (1570 MOs), which are unfortunately still completely intractable at the OVGF level. Very clearly, anthanthrene represents an extremely difficult challenge to quantum chemists.

As with all PAH compounds studied so far, the agreement between the OVGF/cc-pVDZ one-electron ionization energies and experimental results improves rather rapidly with increasing

TABLE 7: Main Results of the OVGF and ADC(3) Calculations on Anthanthrene (C_{2h} Symmetry Point Group)[a]

level	MO	type	HF/6-31G	ADC(3)/6-31G	OVGF/ 6-31G	OVGF/cc-pVDZ	exptl[b]
1	$6a_u$	π	6.038	5.931 (0.839)	5.928 (0.880)	6.313 (0.876)	6.92
2	$5a_u$	π	8.006	7.545 (0.826)	7.427 (0.883)	7.709 (0.879)	8.08
3	$5b_g$	π	8.356	7.786 (0.825)	7.665 (0.877)	7.935 (0.872)	8.22
4	$4b_g$	π [s_1][e]		7.422 (0.089)[d]			
4	$4b_g$	π	9.258	8.608 (0.759)[d]	8.318 (0.839)[d]	8.589 (0.829)[d]	8.5[c]
5	$3b_g$	π	10.230	9.015 (0.632)[d]	9.049 (0.829)[d]	9.353 (0.815)[d]	9.3[c]
5	$3b_g$	π [s_4][e]		9.909 (0.100)[d]			
5	$3b_g$	π [s_5][e]		10.052 (0.053)[d]			
6	$4a_u$	π [s_2][e]	10.104	8.773 (0.172)[d]			
6	$4a_u$	π		9.229 (0.692)[d]	9.012 (0.862)	9.242 (0.856)	9.42
7	$3a_u$	π [s_3][e]		9.598 (0.096)[d]			
7	$3a_u$	π	11.554	10.327 (0.534)[d]	10.194 (0.829)[d]	10.452 (0.818)[d]	10.34
8	$2a_u$	π	12.512	10.573 (0.449)[d]	10.799 (0.801)[d]	11.054 (0.788)[d]	
9	$31a_g$	σ	12.401	10.650 (0.891)	10.349 (0.895)	10.647 (0.886)	10.7[c]
10	$30a_g$	σ	12.615	10.800 (0.888)	10.478 (0.893)	10.761 (0.884)	11.0[c]
11	$2b_g$	σ		10.503 (0.100)[d]			
11	$2b_g$	π	13.255	11.538 (0.336)[d]	11.473 (0.694)[d]	11.711 (0.638)[d]	
12	$30b_u$	σ	13.364	11.515 (0.872)	11.243 (0.883)	11.514 (0.873)	11.6[c]
13	$29b_u$	σ	13.848	11.952 (0.857)	11.703 (0.876)	11.954 (0.865)	12.0[c]
14	$28b_u$	σ	14.484	12.528 (0.870)	12.265 (0.882)	12.477 (0.873)	12.3[c]
15	$29a_g$	σ	14.557	12.578 (0.837)	12.379 (0.868)	12.615 (0.858)	12.3[c]
16	$1b_g$	π	14.304	12.771 (0.173)[d]	12.356 (0.497)[d]	*d*	
17	$28a_g$	σ	14.979	13.000 (0.858)	12.766 (0.876)	12.959 (0.866)	12.9[c]
18	$27b_u$	σ	15.125	13.182 (0.637)	12.983 (0.868)	13.206 (0.859)	12.9[c]
19	$1a_u$	π	15.577	12.962 (0.079)	13.272 (0.701)[d]	13.435 (0.656)[d]	
20	$26b_u$	σ	15.383	13.309 (0.830)	13.105 (0.867)	13.295 (0.857)	
21	$27a_g$	σ	15.755	13.654 (0.813)	13.503 (0.872)	13.645 (0.864)	13.5[c]
22	$26a_g$	σ	15.928	13.759 (0.825)	13.443 (0.868)	13.629 (0.857)	13.5[c]
23	$25b_u$	σ	16.303	14.089 (0.830)	13.831 (0.865)	13.973 (0.855)	13.8[c]
24	$25a_g$	σ	16.512	14.264 (0.791)	14.025 (0.861)	14.170 (0.852)	
25	$24a_g$	σ	16.950	14.702 (0.621)[d]	14.573 (0.857)[d]	14.744 (0.846)[d]	14.7[c]
26	$24b_u$	σ	17.323	15.095 (0.481)[d]	14.957 (0.853)[d]	15.006 (0.833)[d]	14.9[b]
27	$23b_u$	σ	17.524	15.138 (0.366)[d]	14.982 (0.850)[d]	15.062 (0.828)[d]	14.9[c]
28	$23a_g$	σ	17.998	15.365 (0.209)[d]	15.466 (0.835)[d]	15.536 (0.822)[d]	15.4[c]
29	$22b_u$	σ	18.909	16.443 (0.230)[d]	16.213 (0.818)[d]	*d*	
30	$22a_g$	σ	19.157	16.589 (0.122)[d]	*d*	*d*	
31	$21b_u$	σ	19.329	16.863 (0.112)[d]	*d*	*d*	
32	$21a_g$	σ	19.427	16.689 (0.110)[d]	*d*	*d*	
33	$20b_u$	σ	20.477	17.709 (0.126)[d]	*d*	*d*	
34	$20a_g$	σ	21.198	18.191 (0.064)[d]	*d*	*d*	

[a] Binding energies are given in eV, along with the associated pole strengths (Γ's) in brackets. [b] Boschi, R.; Clar, E.; Schmidt, W. *J. Chem. Phys.* **1974**, *60*, 4406. [c] My assignment. [d] Breakdown of the molecular orbital picture of ionization. At binding energies larger than 10.0 eV, only the most intense ADC(3)/6-31G ionization lines are given here; see Table 8 for further data. [e] [s_x] dominant shake-up configuration: $s_1 = 6a_u^{-2}\ 6b_g^{+1}$; $s_2 = 6a_u^{-2}\ 7a_u^{+1}$; $s_3 = 6a_u^{-1}\ 4b_g^{-1}\ 6b_g^{+1}$; $s_4 = 6a_u^{-2}\ 8b_g^{+1}$; $s_5 = 6a_u^{-2}\ 7b_g^{+1}$; $s_6 = 6a_u^{-2}\ 7b_g^{+1}$

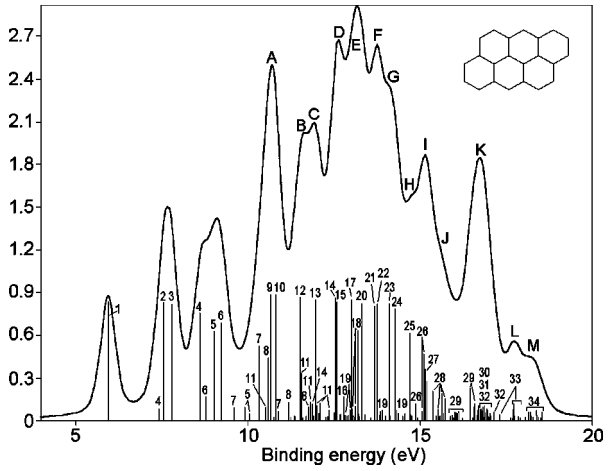

Figure 8. ADC(3)/6-31G spike and convoluted ionization spectra of anthanthrene (fwhm = 0.5 eV).

binding energies. Ionization of the $5a_u$ (**2**) and $5b_g$ (**3**) orbitals is described within accuracies of 0.37 and 0.28 eV in terms of one-electron processes at the OVGF/cc-pVDZ level ($\Gamma > 0.85$), a picture which the ADC(3)/6-31G results fully support. A breakdown of the orbital picture of ionization can be anticipated from the pole strengths found at the OVGF/cc-pVDZ level ($\Gamma < 0.83$) for the $4b_g$ (**4**) and $3b_g$ (**5**) orbitals, a prediction which the ADC(3)/6-31G results confirm for both levels (in both cases, a satellite with a pole strength around 0.1 is found). In the He(I) spectrum (Figure 9), the band (**2**−**4**) peaking at 8.08, 8.22, and 8.5 eV exhibits a very long tail extending from 8.5 to 9.0 eV, possibly indicating unusually strong vibronic interactions. The shoulder at 9.3 eV and the peak at 9.42 eV in the He(I) spectrum (Figure 9) can be confidently ascribed to the most intense lines originating from ionization of the $3b_g$ (**5**) and $4a_u$ (**6**) orbitals, respectively. Beyond this point, the shake-up fragmentation intensifies, and the OVGF approach is no longer valid in the π-band system. With regard to its sharp appearance and relative location, the peak at a binding energy of 10.34 eV in the He(I) spectrum can only be related to the most intense line ($\Gamma = 0.53$) derived at the ADC(3)/6-31G level from the $3a_u$ π-orbital (**7**).

The outermost one-electron ionization lines in the σ-band system of anthanthrene are reached with the (relatively broader) peaks at 10.7 and 11.0 eV, which derive from orbitals $31a_g$ and $30a_g$ (**9**, **10**). In that system, the one-electron picture of ionization remains valid up to binding energies of 14.8 eV (Table 7). Therefore, the peaks (**B**−**F**) at binding energies of 11.6, 12.0, 12.3, 12.9, and 13.5 eV in the He(I) spectrum can be ascribed

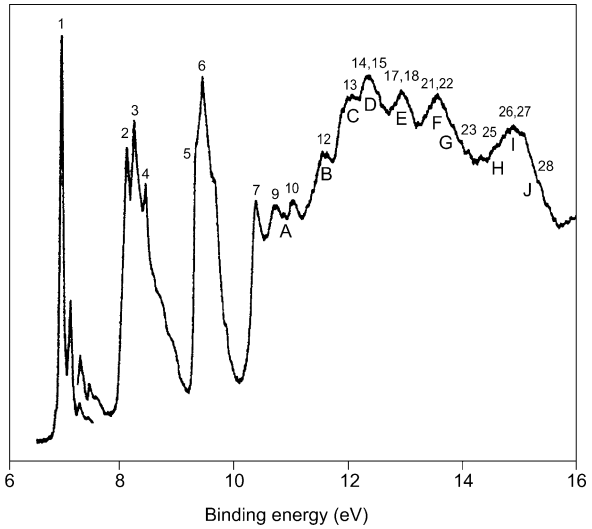

Figure 9. Gas-phase He(I) photoemission spectrum of anthanthrene (adapted from ref 26).

within an accuracy of 0.3 eV at the OVGF/cc-pVDZ level to the $30b_u$ (**12**), $29b_u$ (**13**), {$28b_u$ (**14**) + $29a_g$ (**15**)}, {$28a_g$ (**17**) + $27b_u$ (**18**) + $26b_u$ (**20**)}, and {$27a_g$ (**21**) + $26a_g$ (**22**)} orbital subsets, respectively. Also, the ionization of an electron in orbital $25b_u$ (**23**) yields one line corresponding to the shoulder (**G**) seen at 13.9 eV in the experimental spectrum. A partial breakdown of the orbital picture of ionization is observed for orbital $24a_g$ (**25**), whose most significant contribution to the ADC(3)/6-31G spectrum is a line at 14.7 eV with a pole strength of 0.62. By comparison with the simulation displayed in Figure 8, this line can be related to a shoulder (**H**) at ~14.6 eV on the experimental side (Figure 9). The peak (**I**) at 14.9 eV in the He(I) spectrum is then ascribed to a dense set of lines originating from the ionization of orbitals $24b_u$ (**26**) and $23b_u$ (**27**). The ionization of orbital $23a_g$ (**28**) yields a series of shake-up lines at binding energies ranging from 15.3 to 16.0 eV, which fit well with the shoulder (**J**) seen experimentally at ~15.6 eV (Figure 9). Proceeding further with the ADC(3)/6-31G spectrum only (Figure 8, Tables 7 and 8), one intense peak (**K**) culminating at ~16.8 eV is predicted from the shake-up ionization energies pertaining to orbitals $22b_u$ (**29**), $22a_g$ (**30**), $21b_u$ (**31**), and $21a_g$ (**32**). This peak marks the border between the outer- and inner-valence regions of anthanthrene, the latter two orbitals being molecular orbitals dominated by C_{2s} atomic contributions. Ionization of the $20b_u$ (**33**) and $20a_g$ (**34**) orbitals yields two further shake-up bands (**L**, **M**) at binding energies of ~17.7 and ~18.1 eV, respectively (Figure 8, Tables 7 and 8).

The ADC(3)/6-31G results are overall in line with the TDDFT (BLYP) calculations by Hirata et al. of the lowest excited states of the radical cation of anthanthrene in its ground state (^2A_u).[31] According to these TDDFT calculations, the lowest excitation energies of anthanthrene$^+$ amount to 1.19, 1.31, 1.89, 2.31, and 2.33 eV. In the same order, these correspond to [$\pi_0^* \leftarrow \pi_{-x}$] doublet−doublet transitions belonging to the A_u, B_g, B_g, B_g, and A_u irreducible representations of the C_{2h} point group. This is consistent with the ADC(3)/6-31G results, which locate the most intense lines resulting from ionization of the $5a_u$ (**2**), $5b_g$ (**3**), $4b_g$ (**4**), $3b_g$ (**5**), and $4a_u$ (**6**) π-orbitals at 1.61, 1.86, 2.68, 3.08, and 3.30 eV above the ionization threshold, respectively. For these lines, in view of the strong underestimation of the ionization threshold, the agreement with the TDDFT (BLYP)/6-31G** results would certainly improve if the ADC(3) calculations could be performed with a larger basis set. For instance, at the OVGF/cc-pVDZ level, the $5a_u^{-1}$ (**2**), $5b_g^{-1}$ (**3**), and $4a_u^{-1}$ (**6**) one-electron ionization lines fall at 1.40, 1.62, and 2.93 eV above the $6a_u^{-1}$ reference (**1**), to compare with experimental energy intervals of 1.16, 1.30, and 2.50 eV, and, correspondingly, TDDFT (BLYP)/6-31G** excitation energies of 1.19, 1.31, and 2.33 eV (vide supra).

Both the ADC(3)/6-31G and TDDFT (BLYP)/6-31G** results indicate that the lowest shake-up state (s_1) of anthanthrene corresponds to the $6a_u^{-2}$ $6b_g^{+1}$ (HOMO^{-2} LUMO^{+1}) configuration and has a B_g symmetry label. The relative energy location of this shake-up transition is not entirely clear, however. At the ADC(3)/6-31G level, the ^2B_g [$\pi_1^* \leftarrow \pi_0$] state represents the first excited state of anthanthrene$^+$, at 1.50 eV above the ^2A_u cation ground state, whereas an excitation energy of 2.50 eV is correspondingly found at the TDDFT (BLYP)/6-31G** level.[31] With both approaches, the second ionized shake-up state of anthanthrene (s_2) is a ^2A_u state which corresponds to the $6a_u^{-1}$ $5a_u^{-1}$ $6b_g^{+1}$ electronic configuration. In the ADC(3)/6-31G spectrum, this state is found at 2.84 eV above the ionization threshold, which is, this time, fully consistent with the excitation energy (3.02 eV) that has been correspondingly reported for

TABLE 8: Further Ionization Lines Identified at the ADC(3)/6-31G Level for Anthanthrene (C_{2h} Symmetry Point Group)[a]

level	MO	type	ADC(3)/6-31G
7	$3a_u$	π	10.879 (0.081), 11.213 (0.069), 11.263 (0.054)
8	$2a_u$	π	11.168 (0.133), 11.343 (0.041), 11.591 (0.024), 11.758 (0.104),11.890 (0.036), 12.067 (0.057), 12.312 (0.031), 13.566 (0.023)
11	$2b_g$	π	10.503 (0.100), 11.256 (0.025), 11.366 (0.035), 11.878 (0.116), 12.086 (0.130), 12.253 (0.026), 12.503 (0.059), 12.823 (0.042)
16	$1b_g$	π	11.810 (0.134), 11.985 (0.114), 11.687 (0.034), 12.349 (0.074), 12.666 (0.043), 13.051 (0.037), 13.088 (0.027), 13.195 (0.051), 13.388 (0.030), 14.488 (0.030)
18	$27b_u$	σ	13.029 (0.088), 13.127 (0.104)
19	$1a_u$	π	12.688 (0.048), 12.786 (0.038), 12.884 (0.037), 12.920 (0.042), 13.225 (0.033), 13.391 (0.043), 13.753 (0.067), 13.846 (0.065), 13.902 (0.072), 14.001 (0.032), 14.127 (0.033), 14.311 (0.072)
21	$27a_g$	σ	13.824 (0.037)
25	$24a_g$	σ	14.368 (0.051), 14.559 (0.049), 15.187 (0.085)
26	$24b_u$	σ	14.721 (0.043), 14.764 (0.032), 14.855 (0.118), 14.911 (0.021), 15.637 (0.046), 15.676 (0.053), 15.876 (0.034)
27	$23b_u$	σ	15.186 (0.283), 14.734 (0.031), 15.052 (0.069), 15.521 (0.035), 15.961 (0.022)
28	$23a_g$	σ	15.627 (0.195), 15.719 (0.157), 15.464 (0.037), 15.504 (0.078), 15.939 (0.040), 16.001 (0.061)
29	$22b_u$	σ	16.031 (0.060), 16.126 (0.071), 16.432 (0.224), 16.642 (0.043), 16.737 (0.085)
30	$22a_g$	σ	15.552 (0.026), 16.559 (0.106), 15.582 (0.037), 16.544 (0.044), 16.556 (0.033), 16.702 (0.047), 16.768 (0.092), 16.822 (0.092), 16.872 (0.020), 16.960 (0.077), 17.018 (0.059), 17.056 (0.035)
31	$21b_u$	σ	16.079 (0.055), 16.532 (0.023), 16.571 (0.104), 16.583 (0.045), 16.672 (0.042), 16.852 (0.024), 16.822 (0.103), 16.874 (0.060), 16.942 (0.086), 16.966 (0.029), 16.984 (0.032)
32	$21a_g$	σ	16.218 (0.020), 16.662 (0.076), 16.792 (0.072), 16.858 (0.034), 16.910 (0.031), 16.932 (0.091), 16.981 (0.022), 17.036 (0.041), 17.144 (0.064)
33	$20b_u$	σ	17.313 (0.049), 17.630 (0.029), 17.659 (0.022), 17.695 (0.086), 17.742 (0.038), 17.753 (0.033), 17.837 (0.033), 17.899 (0.028)
34	$20a_g$	σ	18.053 (0.030), 18.133 (0.065), 18.191 (0.064), 18.210 (0.039), 18.268 (0.031), 18.385 (0.045), 18.531 (0.064)

[a] Binding energies are given in eV, along with the associated pole strengths (Γ's) in brackets.

anthanthrene$^+$ at the TDDFT (BLYP)/6-31G** level. The ADC(3)/6-31G (OVGF/cc-pVDZ) results place the σ-ionization threshold (**9**) at 4.72 eV (4.33 eV) above the first ionization line of anthanthrene, to compare with an experimental energy interval of 3.78 eV and, once more, a much too low TDDFT (BLYP)/6-31G** estimation of 3.03 eV for the first ^2A_g [$\pi_0^* \leftarrow \sigma$] excitation energy of anthanthrene$^+$.[31] Again, because of such a severe underestimation, Hirata et al. have erroneously ascribed the σ-ionization onset of anthanthrene to the peak at a binding energy of 10.34 eV (**7**), at 3.42 eV above the ionization threshold.

Concluding Remarks

The OVGF/cc-pVDZ level predicts the outer-valence one-electron ionization energies of large polycyclic benzenoid hydrocarbon compounds to within 0.3 eV of the experimental data, with the exception of the very first ionization energies, for which discrepancies up to ~0.6 eV are noted when tackling systems with enhanced polyenic character and, thus, lower aromaticity, higher reactivity, lower band gap, and thus a more strongly correlated nature, such as in anthanthrene or large oligoacenes.[29] These enhanced discrepancies are not to be imputed to deficiencies of the OVGF approach but to an exacerbated dependency of the outermost ionization energies of low band-gap systems on the quality of the basis set.[51] The OVGF/6-31G and OVGF/cc-pVDZ data reported in this work demonstrate that the sensitivity of the one-electron binding energies to the basis set decreases with increasing binding energies. The reason is that, for the outermost levels, the leading second-order corrections to orbital binding energies are pair-removal corrections,[59] which arise from the particle component of the self-energy and imply double electronic excitations across the fundamental band gap, whereas at higher binding energies, the orbital and pair relaxation terms[59] linked to the hole component of the second-order self-energy predominate[60] (these terms only require single excitations over the fundamental band gap, along with a relaxation of the hole within occupied levels, and are thus naturally much less sensitive to the description of unoccupied levels). In view of the dependence of the π-ionization thresholds of PAH compounds on the quality of the basis set,[51] and the excellent agreement between results obtained at the OVGF and benchmark CCSD(T) levels (see Table 9 in ref 51), an overall accuracy between ~0.1 eV and ~0.2 eV on one-electron binding energies should be reached with the OVGF, and by extension, ADC(3) approaches, in the limit of an asymptotically complete basis set. Comparison with ADC(3)/6-31G and OVGF/6-31G results shows that, at the OVGF/cc-pVDZ level, there is no ambiguity on the energy order of one-electron ionization states and, in particular, on the relative energy location of the σ-onset.

Nowadays, in one-particle Green's function calculations performed using a diagonal self-energy (quasiparticle approximation) such as OVGF, pole strengths larger than 0.80 are assumed to validate the one-electron picture of ionization.[61] However, a comparison of OVGF/cc-pVDZ and ADC(3)/6-31G results confirms the empirical rule[30] that OVGF/cc-pVDZ pole strengths smaller than 0.85 systematically corroborate a breakdown of the orbital picture of ionization, at the ADC(3)/6-31G level. This threshold of 0.85 on OVGF pole strengths should thus be regarded as the red line below which OVGF ionization energies (and by extrapolation any electron binding energy obtained within the framework of a one-electron or quasiparticle depiction) are most certainly meaningless and should be proscribed. Care is still needed even when the OVGF pole strengths remain larger than 0.85, especially around the shake-up onset of extended conjugated systems, which appears to be extremely sensitive to the employed theoretical approach. Despite the obvious limitations of the 6-31G basis set, as well as the extent of the satellite bands, both in the π- and σ-band systems, the simulated ADC(3) one-electron and shake-up ionization spectra are in excellent agreement with the available UV He(I) photoemision and He*(2^3S) Penning ionization spectra, up to binding energies of 16 eV. It would be worth measuring the electron momentum, UV He(II) or X-ray photoionization spectra of the title compounds, to study in detail the bands that exclusively relate to shake-up and shake-off transitions, at binding energies larger than ~16 eV.

Besides providing consistent insights into the He(I) spectra of the title compounds, the present results are also, overall, in line with TDDFT studies of the low-lying [$\pi^* \leftarrow \pi$] excited states of the corresponding radical cations and favorably support the comparison with experimental doublet−doublet excitation energies in the related radical cations. The main drawback on the side of the 1p-GF calculations is, again, the sensitivity of the ionization threshold of the neutral molecules to the quality of the basis set. As the employed basis sets (6-31G, cc-pVDZ) are far from being complete, the ionization threshold is systematically underestimated and, quite naturally, therefore, the excitation energies in the cation are systematically overestimated. TDDFT easily circumvents this difficulty, by ascribing the ionization thresholds of the neutral molecules to the zero of excitation energies in the cations. On the other hand, the currently employed exchange-correlation functionals, among which is BLYP, are known to suffer from more fundamental deficiencies, such as an overestimated localization of the exchange-correlation hole, an incomplete cancellation of the self-interaction, and a too-rapid decay of the corresponding potentials in the asymptotic region.[62] As a consequence, TDDFT yields substantial errors in valence excitation energies for the valence-excited states of large π-conjugated molecules[63] and for charge transfer (CT) processes.[64−66] Especially, underestimations up to 7.5 and 2.4 eV have been noted for long-range CT excitation energies in cofacial ethylene−tetrafluoroethylene[65] and zinc-bacteriochlorin−bacteriochlorin complexes,[66] respectively. In the present study, it has been found that, compared to the OVGF/cc-pVDZ estimates of excitation energies in the PAH radical cations, the TDDFT (BLYP)/6-31G** level also yields systematic and significant underestimations, between ~0.9 and ~1.3 eV, of the lowest [$\pi_0^* \leftarrow \sigma$] transition energies. These underestimations are far too large to be imputed to the incompleteness of the employed basis sets only and have undoubtedly led to erroneous identifications[31] of the σ-ionization onset in the photoemission spectra of the neutral molecules. The [$\pi_0^* \leftarrow \sigma$] transitions of PAH radical cations obviously involve an extensive spatial reorganization of the one-electron density, and the origin of such large underestimations can thus also partly be ascribed to the previously listed deficiencies of the standard exchange-correlation BLYP functional.

Acknowledgment. M.S.D. acknowledges financial support from the Fonds voor Wetenschappelijk Onderzoek van Vlaanderen, the Flemish branch of the Belgian National Science Foundation, and from the Bijzonder Onderzoeks Fonds of the Limburgs Universitair Centrum (LUC), Belgium. M.S.D is indebted to Prof. J.-P. François (LUC, Belgium) for support and careful reading.

References and Notes

(1) *Polycyclic Aromatic Hydrocarbons and Astrophysics*; Leger, A., D'hendecourt, L., Boccara, N., Eds.; Reidel: Dordrecht, The Netherlands, 1987.

(2) (a) Crawford, M. K.; Tielens, A. G. G. M.; Allamandola, L. J. *Astrophys. J.* **1985**, *293*, L45. (b) Allamandola, L. J.; Sanford, S. A.; Wopencka, B. *Science* **1987**, *237*, 56. (c) Allamandola, L. J.; Tieles, A. G. G. M.; Barker, J. R. *Astrophys. J. Suppl. Ser.* **1989**, *71*, 733. (d) Puget, J. L.; Leger, A. *Annu. Rev. Astron. Astrophys.* **1989**, *27*, 161. (e) Allamandola, L. J. *Top. Curr. Chem.* **1990**, *1* (f) Salama, F.; Allamandola, L. J. *Astrophys. J.* **1992**, *395*, 301. (g) Bohme, D. K. *Chem. Rev.* **1992**, *92*, 1487. (h) Salama, F.; Allamandola, L. J. *J. Chem. Soc., Faraday Trans.* **1993**, *89*, 2277. (i). DeFrees, J.; Miller, M. D.; Talbi, D.; Pauzat, F.; Ellinger, Y. *Astrophys. J.* **1993**, *408*, 503. (j) Clemett, S. J.; Maechling, C. R.; Zare, R. N.; Swan, P. D.; Walker, R. M. *Science* **1993**, *262*, 721. (k) Salama, F.; Joblin, C.; Allamandola, L. J. *J. Chem. Phys.* **1994**, *101*, 10252. (l) Langhoff, S. R. *J. Phys. Chem.* **1996**, *100*, 2819. (m) Allamandola, L. J.; Hudgins, D. M.; Sanford, S. A. *Astrophys. J.* **1999**, *511*, L115. (n) Duley, W. W.; Seahra, S. S. *Astrophys. J.* **1999**, *522*, L129. (o) Hudgins, D. M.; Bauschlicher, C. W.; Allamandola, L. J.; Fetzer, J. C. *J. Phys. Chem. A* **2000**, *104*, 3655.

(3) (a) Szczepanski, J.; Vala, M. *Astrophys. J.* **1993**, *414*, 646. (b) Szczepanski, J.; Vala, M. *Nature* **1993**, *363*, 699. (c) Hudgins, D. M.; Sandford, S. A.; Allamandola, L. J. *J. Phys. Chem.* **1994**, *98*, 4243. (d) Hudgins, D. M.; Allamandola, L. J. *J. Phys. Chem.* **1995**, *99*, 8978.

(4) (a) Sellgren, K.; Brooke, T. Y.; Smith, R. G.; Geballe, T. R. *Astrophys. J.* **1995**, *449*, L69. (b) Brooke, T. Y.; Sellgren, K.; Geballe, T. R.; *Astrophys. J.* **1999**, *517*, 883. (c) Bregman, J. D.; Hayward, T. L.; Sloan, G. C. *Astrophys. J.* **2000**, *544*, L75. (d) Chiar, J. E.; Tielens, A. G. G. M.; Whittet, D. C. B.; Schutte, W. A.; Boogert, A. C. A.; Lutz, D.; van Dishoeck, E. F.; Bernstein, M. P. *Astrophys. J.* **2000**, *537*, 749.

(5) Sephton, M. A.; Love, G. D.; Watson, J. S.; Verchovsky, A. B.; Wright, I. P.; Snape, C. E.; Gilmour, I. *Geochim. Cosmochim. Acta* **2004**, *68*, 1385.

(6) Bernstein, M. P.; Dworkin, J. P.; Sanford, S. A.; Allamandola, L. J. *Adv. Space Res.* **2002**, *1510*, 30.

(7) Hopf, H. *Classics in Hydrocarbon Chemistry*; Wiley-VCH: Weinheim, Germany, 2000.

(8) Frundental, R. I.; Jones, P. W. *Polynuclear Aromatic Hydrocarbons*; Raven: New York, 1976.

(9) *Calculated Properties of Polycyclic Aromatic Hydrocarbons*; Hites, R. A., Simonsick, W. J., Jr., Eds.; Elsevier: New York, 1987.

(10) *Understanding our Environment: An Introduction to Environmental Chemistry and Pollution*, 2nd ed.; Harrison, R. M., Ed.; Royal Society of Chemistry: Cambridge, U.K., 1992.

(11) Busch, H. *The Molecular Biology of Cancer*; Academic: New York, 1974.

(12) Ahrens, J.; Keller, A.; Kovacs, R.; Homann, K.-H. *Ber. Bunsen-Ges. Phys. Chem.* **1998**, *102*, 1823 and references therein.

(13) Fang, M.; Zheng, M.; Wang, F.; To, K. L.; Jaafar, A. B.; Tong, S. L. *Atmos. Environ.* **1999**, *33*, 783.

(14) Bauer, S. H.; Jeffers, P. M. *Energy Fuels* **1988**, *2*, 446.

(15) Kroto, H. W.; Fischer, J. E.; Cox, D. E. *The Fullerenes*; Pergamon: Oxford, U.K., 1993.

(16) (a) Kroto, H. W.; Alaf, A. W.; Balm, S. P. *Chem. Rev.* **1991**, *91*, 1213. (b) Curl, R. F. *Nature* **1993**, *363*, 14.

(17) Verlaak, S.; Steudel, S.; Heremans, P.; Janssen, D.; Deleuze, M. S. *Phys. Rev. B* **2003**, *68*, 195409.

(18) (a) Minakata, T.; Imai, H.; Ozaki, M. *J. Appl. Phys.* **1992**, *72*, 4178. (b) Brown, A. R.; Pomp, A.; Hart, C. M.; de Leeuw, D. M. *Science* **1995**, *270*, 972. (c) Dodobalapur, A.; Laquidanum, J.; Katz, H. E.; Bao, Z. *Appl. Phys. Lett.* **1996**, *69*, 4227. (d) Dimitrakopoulos, C. D.; Purishotoman, S.; Kymissis, J.; Callegari, A.; Shaw, J. M. *Science* **1999**, *283*, 822. (e) Verlaak, S.; Arkhipov, V.; Heremans, P. *Appl. Phys. Lett.* **2003**, *82*, 745.

(19) *Organic Electronic Materials: Conjugated Polymers and Low Molecular Weight Solids*; Farchioni, R., Grosso, G., Eds.; Springer: New York, 2001.

(20) (a) Fetzer, S. M.; Huang, C.-R.; Harvey, R. G.; LeBreton, P. R. *J. Phys. Chem.* **1993**, *97*, 2385. (b) Dabestani, R.; Ivanov, I. N. *Photochem. Photobiol.* **1999**, *70*, 10.

(21) Pope, C. J.; Marr, J. A.; Howard, J. B. *J. Phys. Chem.* **1993**, *97*, 11001.

(22) See, for example, (a) Szczepanski, J.; Vala, M.; Talbi, D.; Parisel, O.; Ellinger, Y. *J. Chem. Phys.* **1993**, *98*, 4494. (b) Negri, F.; Zgierski, M. Z. *J. Chem. Phys.* **1994**, *100*, 1387. (c) Niederalt, C.; Grimme, S.; Peyerimhoff, S. D. *Chem. Phys. Lett.* **1995**, *245*, 455. (d) Vala, M.; Szczepanski, J.; Pauzat, F.; Parisel, I.; Talbi, D.; Ellinger, Y. *J. Phys. Chem.* **1994**, *98*, 9187. (e) Bally, T.; Carra, C.; Fülscher, M. P.; Zhu, Z. *J. Chem. Soc., Perkin Trans. 2* **1998**, 1759. (f) Hirata, S.; Lee, T. J.; Head-Gordon, M. *J. Chem. Phys.* **1999** *111*, 8904. (g) Halasinski, T. M.; Hudgins, D. M.; Salama, F.; Allamandola, L.; Bally, T. *J. Phys. Chem. A* **2000**, *104*, 7484 and references therein.

(23) (a) Clark, L. B. *J. Chem. Phys.* **1965**, *43*, 2566. (b) Kitagawa, T.; Inokuchi, H.; Kodera, K. *J. Mol. Spectrosc.* **1966** *21*, 267. (c) Kitagawa, T. *J. Mol. Spectrosc.* **1968**, *26*, 1. (d) Eland, J. H. D.; Dandy, C. J. *Z. Naturforsch., A: Phys. Sci.* **1968**, *23*, 355. (e) Dewar, M. J. S.; Worley, D. S. *J. Chem. Phys.* **1969**, *51*, 263. (f) Clark, P. A.; Brogli, F.; Heilbronner, E. *Helv. Chim. Acta* **1972**, *55*, 1415. (g) Brogli, F.; Heilbronner, E. *Angew. Chem.* **1972**, *84*, 551. (h) Brogli, F.; Heilbronner, E. *Theor. Chim. Acta* **1972**, *26*, 289. (i) Ruscic, B.; Kovac, B.; Klasinc., L.; Gusten, H. *Z. Naturforsch., A: Phys. Sci.* **1974**, *33*, 1006. (j) Streets, D. G.; Williams T. A. *J. Electron Spectrosc. Relat. Phenom.* **1974**, *3*, 71. (k) Hush, N. S.; Cheung, A. S.; Hilton, P. R. *J. Electron Spectrosc. Relat. Phenom.* **1975**, *7*, 383. (l) Obenland, S.; Schmidt, W. *J. Am. Chem. Soc.* **1975**, *97*, 6633. (m) Schmidt, W. *J. Chem. Phys.* **1977**, *66*, 828. (n) Riga, J. J.; Pireaux, J. J.; Caudano, R.; Verbist, J. J. *Phys. Scr.* **1977**, *16*, 346. (o) Munakata, T.; Ohno, K.; Harada, Y.; Kuchitsu, K. *Chem. Phys. Lett.* **1981**, *83*, 243. (p) Boutique, J.-P.; Riga, J.; Verbist, J. J.; Delhalle, J.; Fripiat, J. G. *J. Electron Spectrosc. Relat. Phenom.* **1984**, *33*, 243. (q) Kajiwara, T.; Masuda, S.; Ohno, K.; Harada, Y. *J. Chem. Soc., Perkin Trans.* **1988**, *2*, 507. (r) Weber, P. M.; Thantu, N. *Chem. Phys. Lett.* **1992**, *197*, 556. (s) Zakrzewski, V. G.; Dolgounitcheva, O.; Ortiz, J. V. *J. Chem. Phys.* **1996**, *105*, 8748. (t) Zakrzewski, V. G.; Dolgounitcheva, O.; Ortiz, J. V. *J. Chem. Phys.* **1997**, *107*, 7906. (u) Yamauchi, M.; Yamakita, Y.; Yamakado, H.; Ohno, K. *J. Electron Spectrosc. Relat. Phenom.* **1998**, *88*, 155. (v) Dolgounitcheva, O.; Zakrzewski, V. G.; Ortiz, J. V. *J. Phys. Chem. A* **2000**, *104*, 10032. (w) Zakrzewski, V. G.; Dolgounitcheva, O.; Ortiz, J. V. *Int. J. Quantum Chem.* **2000**, *80*, 836. (x) Ozaki, H. *J. Chem. Phys.* **2000**, *113*, 6361. (y) Koch, N.; Ghijsen, J.; Johnson, R. L.; Schwartz, J.; Pireaux, J.-J.; Kahn, A. *J. Phys. Chem. B* **2002**, *106*, 4192. (z) Koch, N.; Kahn, A.; Ghijsen, J.; Pireaux, J.-J.; Schwartz, J.; Johnson, R. L.; Elschner, A. *Appl. Phys. Lett.* **2003**, *82*, 70.

(24) Boschi, R.; Murrell, J. N.; Schmidt, W. *Discuss. Faraday Soc.* **1972**, *54*, 116.

(25) Boschi, R.; Schmidt, W. *Tetrahedron Lett.* **1972**, ***25***, 2577.

(26) Boschi, R.; Clar, E.; Schmidt, W. *J. Chem. Phys.* **1974**, *60*, 4406.

(27) Yanakado, H.; Sawada, Y.; Shinohara, H.; Ohno, K. *J. Electron Spectrosc. Relat. Phenom.* **1998**, *88*−*91*, 927.

(28) (a) Deleuze, M. S.; Cederbaum, L. S. *Phys. Rev. B* **1996**, *53*, 13326. (b) Deleuze, M. S.; Cederbaum, L. S. *Int. J. Quantum Chem.* **1997**, *63*, 465. (c) Deleuze, M. S.; Cederbaum, L. S. *Adv. Quantum Chem.* **1999**, *35*, 77. (d) Deleuze, M. S.; Giuffreda, M. G.; François, J.-P.; Cederbaum, L. S. *J. Chem. Phys.* **1999**, *111*, 5851. (e) Deleuze, M. S.; Giuffreda, M. G.; François, J.-P.; Cederbaum, L. S. *J. Chem. Phys.* **2000**, *112*, 5325.

(29) Deleuze, M. S.; Trofimov, A. B.; Cederbaum, L. S. *J. Chem. Phys.* **2001**, *115*, 5859.

(30) Deleuze, M. S. *J. Chem. Phys.* **2002**, *116*, 7012.

(31) Hirata S.; Head-Gordon, M.; Szczepanski, J.; Vala, M. *J. Phys. Chem. A* **2003**, 107, 4940.

(32) Bauernschmitt, R.; Ahlrichs, R. *Chem. Phys. Lett.* **1996**, *256*, 454.

(33) Kato, T.; Yoshizawa, K.; Yamabe, T. *J. Chem. Phys.* **1999**, *110*, 249.

(34) (a) Deleuze, M. S.; Cederbaum; L. S. *Int. J. Quantum Chem*. **1997**, *63*, 465. (b) Trofimov, A. B.; Schirmer, J.; Holland, D. M. P.; Karlsson, L.; Maripuu, R.; Siegbahn, K.; Potts, A. W. *Chem. Phys.* **2001**, *263*, 167. (c) Potts, A. W.; Holland, D. M. P.; Trofimov, A. B.; Schirmer, J.; Karlsson, L.; Siegbahn, K. *J. Phys. B: At. Mol. Opt. Phys.* **2003**, *36*, 3129.

(35) (a) Gruhn, N. E.; da Sliva Filho, D. A.; Bill, T. G.; Malagoli, M.; Coropceanu, V.; Kahn, A.; Brédas, J.-L. *J. Am. Chem. Soc.* **2002**, *124*, 7918. (b) Keil, M.; Samori, P.; dos Santos, D. A.; Kugler, T.; Stafström, S.; Brand, J. D.; Müllen, Brédas, J.-L.; Rabe, J. P.; Salaneck, W. R. *J. Phys. Chem. B* **2000**, *104*, 3967.

(36) (a) Cornil, J.; Vanderdonckt, S.; Lazzaroni, R.; dos Santos, D. A.; Thys, G.; Geise, H. J.; Yu, L. M.; Szablewski, M.; Bloor, D.; Lögdlund, M.; Salaneck, W. R.; Gruhn, N. E.; Lichtenberger, D. L.; Lee, P. A.; Armstrong, N. R.; Brédas, J.-L. *Chem. Mater.* **1999**, *11*, 2436. (b) Hill, I. G.; Kahn, A.; Cornil, J.; dos Santos, D. A.; Brédas, J.-L. *Chem. Phys. Lett.* **2000**, *317*, 444. (c) Cornil, J.; Gruhn, N. E.; dos Santos, D. A., Malagoli, M.; Lee, P. A.; Barlow, S.; Thayumanavan, S.; Marder, S. R.; Armstrong, N. R.; Brédas, J.-L. *J. Phys. Chem. A* **2001**, 105, 5206. (d) Pascal, L.; Vanden Eyne, J. J.; Van Haverbeke, Y.; Dubois, P.; Michel, A.; Rant, U.; Zojer, E.; Leising, G.; Van Dorn, L. O.; Gruhn, N. E.; Cornil, J.; Brédas, J.-L. *J. Phys. Chem. B* **2002**, 106, 6442.

(37) (a) Schirmer, J.; Cederbaum, L. S.; Walter, O. *Phys. Rev. A* **1983**, *28*, 1237. (b) von Niessen, W.; Schirmer, J.; Cederbaum, L. S. *Comput. Phys. Rep.* **1984**, *1*, 57. (c) Schirmer, J.; Angonoa, G. *J. Chem. Phys.* **1989**, *91*, 1754.

(38) Cederbaum, L. S.; Domcke, W. *Adv. Chem. Phys.* **1977**, *36*, 205.

(39) (a) Öhrn, Y.; Born, G. *Adv. Quantum Chem.* **1981**, *13*, 1. (b) Ortiz, J. V. In *Computational Chemistry: Reviews of Current Trends*; Leszczyinski, J., Ed.; World Scientific: Singapore, 1997; Vol. 2, p 1.

(40) Schirmer, J. *Phys. Rev. A* **1991**, *43*, 4647. (b) Mertins, F.; Schirmer, J. *Phys. Rev. A* **1996**, *53*, 2153.

(41) see Deleuze, M. S. *Int. J. Quantum Chem*. **2003**, *93*, 191 and references therein.

(42) Deleuze, M. S.; Scheller, M. K.; Cederbaum, L. S. *J. Chem. Phys.* **1995**, *103*, 3578.
(43) Golod, A.; Deleuze, M. S.; Cederbaum, L. S. *J. Chem. Phys.* **1999**, *110*, 6014.
(44) The 1p-GF/ADC(3) code originally written by Angonoa, G.; Walter, O.; Schirmer, J.; Cederbaum, L. S.; further developed by Scheller, M. K. and Trofimov, A. B.
(45) Schmidt, M. W.; Baldridge, K. K.; Jensen, J. H.; Koseki, S.; Gordon, M. S.; Nguyen, K. A.; Windus, T. L.; Elbert, S. T. *QCPE Bull.* **1990**, *10*, 52.
(46) Weikert, H.-G.; Meyer, H.-D.; Cederbaum, L. S.; Tarantelli, F. *J. Chem. Phys.* **1996**, *104*, 7122.
(47) (a) Becke, A. D. *J. Chem. Phys.* **1993**, *98*, 5648. (b) Lee, C.; Yang, W.; Parr, R. G. *Phys. Rev. B* **1988**, *37*, 785.
(48) (a) Dunning, T. H., Jr. *J. Chem. Phys.* **1989**, *90*, 1007. (b) Kendall, R. A.; Dunning, T. H.; Harrisson, R. J. *J. Chem. Phys.* **1992**, *96*, 6796.
(49) Jaffe, H. H. *Symmetry in Chemistry*; Wiley: New York, 1967.
(50) Taylor, R. P. Accurate Calculations and Calibration. In *Lecture Notes in Quantum Chemistry*, *European Summer School in Quantum Chemistry*; Roos, B. O., Ed.; Springer-Verlag: Berlin, 1991; pp 325−412.
(51) Deleuze, M. S.; Claes, L.; Kyachko, E. S.; François, J.-P. *J. Chem. Phys.* **2003**, *119*, 3106.
(52) Frisch, M. J.; Trucks, G. W.; Schlegel, H. B.; Scuseria, G. E.; Robb, M. A.; Cheeseman, J. R.; Zakrzewski, V. G.; Montgomery, J. A., Jr.; Stratmann, R. E.; Burant, J. C.; Dapprich, S.; Millam, J. M.; Daniels, A. D.; Kudin, K. N.; Strain, M. C.; Farkas, O.; Tomasi, J.; Barone, V.; Cossi, M.; Cammi, R.; Mennucci, B.; Pomelli, C.; Adamo, C.; Clifford, S.; Ochterski, J.; Petersson, G. A.; Ayala, P. Y.; Cui, Q.; Morokuma, K.; Malick, D. K.; Rabuck, A. D.; Raghavachari, K.; Foresman, J. B.; Cioslowski, J.; Ortiz, J. V.; Stefanov, B. B.; Liu, G.; Liashenko, A.; Piskorz, P.; Komaromi, I.; Gomperts, R.; Martin, R. L.; Fox, D. J.; Keith, T.; Al-Laham, M. A.; Peng, C. Y.; Nanayakkara, A.; Gonzalez, C.; Challacombe, M.; Gill, P. M. W.; Johnson, B. G.; Chen, W.; Wong, M. W.; Andres, J. L.; Head-Gordon, M.; Replogle, E. S.; Pople, J. A. *Gaussian 98*, revision A.7; Gaussian, Inc.: Pittsburgh, PA, 1998.
(53) Using symmetry labels that are consistent with standard molecular orientation under the D_{2h} point group, according to the rules stated explicitly in the book by J. Jaffe (ref 49). See also footnote 55 in ref 30.
(54) Khan, Z. H. *Spectrochim. Acta, Part A* **1989**, *45*, 253.
(55) Randic, M. *Chem. Rev.* **2003**, *103*, 3449.
(56) (a) Clar, E. *Polycyclic Hydrocarbons*; Academic Press: London, 1963; Vols. 1 and 2. (b) Clar, E. *The Aromatic Sextet*; J. Wiley & Sons: London, 1972.
(57) Moran, D.; Stahl, F.; Bettinger, F.; Schaefer, H. F., III; Schleyer, P. v. R. *J. Am. Chem. Soc.* **2003**, *125*, 6746.
(58) Aihara, J.-I. *J. Phys. Chem. A* **2003**, *107*, 11553.
(59) (a) Szabo, A.; Ostlund, N. S. *Modern Quantum Chemistry*; McGraw-Hill: New York, 1982. (b) Pickup, B. T.; Goscinski, O. *Mol. Phys.* **1973**, *26*, 1013.
(60) Deleuze, M.; Denis, J.-P.; Delhalle, J.; Pickup, B. T. *J. Phys. Chem.* **1993**, *97*, 5115.
(61) (a) Zakrzewski, V. G.; Ortiz, J. V.; Nichols, J. A.; Heryadi, D.; Yeager, D. L.; Golab, J. T. *Int. J. Quantum Chem.* **1996**, *60*, 29. (b) Ferreira, A. M.; Seabra, G.; Dolgounitcheva, O.; Zakrzewski, V. G.; Ortiz, J. V. In *Quantum Mechanical Prediction of Thermochemical Data*; Cioslowski, J., Ed.; Kluwer: Dordrecht, The Netherlands, 2001; p 131. (c) Ortiz, J. V. *Int. J. Quantum Chem.* **2003**, *95*, 593.
(62) (a) Casida, M. W.; Jamorski, C.; Casida, K. C.; Salahub, D. R. *J. Chem. Phys.* **1998**, *108*, 4439. (b) Tozer, D. J.; Handy, N. C. *J. Chem. Phys.* **1998**, *109*, 10180.
(63) (a) Cai, Z. L.; Sendt, K.; Reimers, J. R. *J. Chem. Phys.* **2002**, *117*, 5543. (b) Reimers, J. R.; Cai, Z.-L.; Bilic, A.; Hush, A. S. *Ann. N. Y. Acad. Sci.* **2003**, *110*, 235.
(64) (a) Tozer, D. J.; Amos, R. D.; Handy, N. C.; Roos, B. J.; Serrano-Andres, L. *Mol. Phys.* **1999**, *97*, 859. (b) Grimme, S.; Parac, M. *ChemPhysChem***2003**, *2*, 293. (c) Soboloewski, A. L.; Domcke, W. *Chem. Phys.* **2003**, *294*, 73. (d) Dreuw, A.; Fleming, G. R.; Head-Gordon, M. *Phys. Chem. Chem. Phys.* **2003**, *5*, 3247. (e) Dreuw, A.; Fleming, G. R.; Head-Gordon, M. *J. Phys. Chem. B* **2003**, *107*, 6500.
(65) Dreuw A.; Weisman, J. L.; Head-Gordon, M. *J. Chem. Phys.* **2003**, *119*, 2943.
(66) Dreuw, A.; Head-Gordon, M. *J. Am. Chem. Soc.* **2004**, *126*, 4007.